Heliyon 10 (2024) e37075

Contents lists available at ScienceDirect

Heliyon

journal homepage: www.cell.com/heliyon

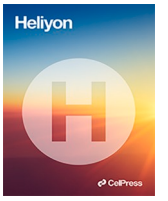

Research article

Extrachromosomal circular DNA-related SPOCK1 contributes to development and enzalutamide resistance of prostate cancer by regulating epithelial mesenchymal transition

Yicong Yao [a,b,1], Qinghua Wang [a,b,1], Wei Jiang [a,b,1], Haopeng Li [a,b], Xilei Li [b], Tong Zi [a,b], Xin Qin [a,b], Yan Zhao [a,b], Denglong Wu [a,**], Gang Wu [a,*]

[a] Department of Urology, Tongji Hospital, School of Medicine, Tongji University, Shanghai, 200065, China
[b] School of Medicine, Tongji University, Shanghai, 200092, China

ARTICLE INFO

Keywords:
eccDNA
Prostate cancer
CRPC
SPOCK1
EMT

ABSTRACT

Prostate cancer is a significant contributor to cancer-related mortality, and the tumor typically develops into castration-resistant prostate cancer (CRPC). Hence, few effective clinical strategies are available to patients with advanced disease. Extrachromosomal circular DNA (eccDNA) is a type of circular DNA originating from the chromosomes but is likely independent of them. Because of its unique structural characteristics, eccDNA has extensive applications as a new biomarker for cancer prevention and treatment. Circle-seq obtains a comprehensive picture of the overall landscape of eccDNA sizes and content in cell populations. In this study, we used Circle-seq and studied the distribution pattern and expression level of eccDNA in prostate cancer. We confirmed that eccDNA is derived from every human chromosome and has sequences from all known types of genomic structures, revealing it is a common mutational element in prostate cancer. We also identified an eccDNA-related gene SPOCK1 that promotes drug resistance, proliferation, and metastasis of many cancers through the epithelial-mesenchymal transition (EMT) mechanism. The SPOCK1-associated eccDNA was highly upregulated in various groups of sequencing results, and SPOCK1 was highly expressed in prostate cancer tissues and cells. Therefore, SPOCK1 exists as eccDNA in prostate cancer and encourages its development and drug resistance via the EMT mechanism. Our results suggest that upregulated genes in the form of eccDNA are oncogenes in prostate cancer and play a pivotal role in carcinogenesis.

1. Introduction

Prostate cancer (PCa) is the second most prevalent cancer in men, accounting for approximately 7 % of newly diagnosed cancer cases worldwide [1,2]. It is also a considerable contributor to cancer-related mortality, causing more than 350,000 deaths annually [3]. Although medical castration is the mainstay treatment for advanced PCa, the tumor ultimately progresses into castration-resistant prostate cancer (CRPC) [4]. Second-generation androgen receptor antagonists, such as enzalutamide (Enz), can prolong patient

* Corresponding author.
** Corresponding author.
E-mail addresses: wudenglong2009@tongji.edu.cn (D. Wu), 2013wg_urologist@tongji.edu.cn (G. Wu).
[1] These authors contributed equally.

https://doi.org/10.1016/j.heliyon.2024.e37075
Received 30 January 2024; Received in revised form 26 August 2024; Accepted 27 August 2024
Available online 16 September 2024

survival but do not prevent PCa progression to the CRPC stage. Hence, in this regard, few effective clinical strategies are available to patients with advanced disease [5].

Extrachromosomal circular DNA (eccDNA) is a type of circular DNA originating from chromosomal DNA but is likely independent of it [6]. This DNA can be observed in normal and cancerous cells, and during cancer progression, it plays a role in cancer initiation, development, and drug resistance by different mechanisms [7]. The unique structural and genetic features of eccDNA provide new clues for cancer surveillance, early diagnosis, treatment, and prediction, having broad application prospects in tumor research [8]. For example, plasma eccDNA has a covalently closed loop structure and is more stable than the linear circulating free DNA, rendering eccDNA a new biomarker for cancer prevention and treatment with broad applications [9,10].

Circularization for in vitro reporting of cleavage effects by sequencing (Circle-seq) is an in vitro screen for identifying genome-wide off-target cleavage sites of CRISPR-Cas9, capturing a comprehensive overall landscape of eccDNA sizes and content in cell populations [11,12]. It has been widely used in eccDNA characterization-related studies of various diseases, such as systemic lupus erythematosus [13], cataracts [14], and gouty arthritis [15]. In this study, Circle-seq and bioinformatics analysis were performed to investigate the distribution pattern and level of eccDNA expression. As a result, the SPARC (osteonectin), cwcv and kazal like domains proteoglycan 1 (SPOCK1) target gene corresponding to the eccDNA with the most pronounced differences in the sequencing results of each group was identified.

The SPARC (osteonectin), cwcv and kazal like domains proteoglycan 1 (SPOCK1) protein is a multi-structural domain proteoglycan that regulates dynamically balanced extracellular mesenchyme (ECM). It is encoded by the SPOCK1 gene, one of the central regulatory genes in the dynamic homeostasis of tumor ECM. It activates many biological processes, such as the epithelial-mesenchymal transition (EMT), causing extracellular matrix remodeling and promoting cell proliferation and invasion [16]. The SPOCK1 gene also uses this mechanism to stimulate drug resistance, proliferation, and metastasis of glioblastoma [17], renal clear cell carcinoma [18], pancreatic cancer [19], and colon cancer [20]. However, the role of this gene in prostate cancer progression and drug resistance has been rarely studied and reported.

In this study, we first examined the differential expression profiles of eccDNA between normal, Enz-sensitive, and Enz-resistant prostate cancer samples. We confirmed that eccDNA is derived from every human chromosome and has sequences from all known types of genomic structures, revealing that eccDNA is a common mutational element in prostate cancer.

We found that SPOCK1-associated eccDNA is highly upregulated in various sequencing results, and SPOCK1 is highly expressed in prostate cancer tissues and cells. We also uncovered that SPOCK1 exists as eccDNA in prostate cancer and promotes its development and drug resistance through the EMT mechanism. Our results suggest that upregulated genes in the form of eccDNA are oncogenes in prostate cancer with a crucial role in carcinogenesis. Importantly, they show that highly expressed genes in the form of eccDNA and their mechanisms of action provide new strategies for treating prostate cancer.

Generally, in this study, we aimed to investigate the role of eccDNAs in the development and enzalutamide resistance of PCa. Particularly, we focused on the distribution pattern and expression level of eccDNAs in the cells and tissues of PCa. Besides, we found that SPOCK1, as one kind of key oncogene, could exist as eccDNA in PCa and encouraged the development and drug resistance of PCa through the EMT mechanism. This mechanism could serve as a molecular basis for the clinical treatment of PCa patients, and provided new perspectives on therapeutic approaches to this disease. Our study laid a solid foundation for this important mechanism.

2. Materials and methods

2.1. Circle-Seq and data analysis

5 kinds of prostate cell lines (i.e., RWPE-1, C4-2, C4-2R, LNCaP, and 22RV1 cells) were collected and lysed to obtain purified high molecular weight DNA. The kit that we used was the Magnetic Animal Tissue Genomic DNA Kit (TIANGEN, DP341). An exonuclease was added to the lysate to eliminate linearized DNA, and its absence was confirmed. The eccDNA-enriched samples were used as a template for phi29 polymerase chain reactions (PCRs), followed by shearing the phi29-amplified DNA with a Bioruptor sonicator. A DNA library was constructed using the purified fragmented DNA and cleaned by beads. The size distribution of DNA fragments was analyzed. The Circle-seq data analysis was performed by DIATRE Biotechnology (Shanghai, China) as follows:

1. The quality of the original data was evaluated using the FastQC software.
2. The original data was compared with the reference genome using the BWA software.
3. The SAM file was processed with Samtools to fit the format required by the Circle-MAP method.
4. The eccDNA was detected with Circle-MAP and genetically annotated.
5. Differential eccDNA analysis and annotated gene function enrichment analysis were performed.

2.2. Western blotting

Cells were lysed with RIPA buffer (Epizyme, Shanghai, China), and total protein concentration was determined by BCA (Bicinchoninic Acid) protein quantification kits (Beyotime, Nantong, China). Equal quantities of total protein were electrophoresed on freshly prepared 10 % sodium dodecyl-sulfate polyacrylamide gels at a voltage of 120 V for 2 h, followed by transferring the proteins onto polyvinylidene fluoride membranes. The membranes were blocked in milk powder solutions for 1 h at room temperature and incubated with the primary antibodies for 12 h at 4 °C. The primary antibodies were as follows: SPOCK1 (Proteintech Group, Inc., 28203-1-AP; 1:1000 dilution), E-cadherin (ABclonal, A22333; 1:1000 dilution), N-cadherin (ABclonal, A19083; 1:500 dilution),

Vimentin (ABclonal, A19607; 1:2000 dilution), N-cadherin (ABclonal, A19083; 1:500 dilution), GAPDH (Abcam plc., ab59164, 1:5000 dilution). The membranes were probed with the secondary antibodies for 2 h at room temperature and visualized using an ECL (Enhanced Chemiluminescence) system.

2.3. Bioinformatics analysis

The SPOCK1 and protein tyrosine phosphatase receptor type N2 (PTPRN2) expression data between tumor and normal prostate tissues were acquired from The Cancer Genome Atlas (TCGA) (http://gdc.cancer.gov) and Gene Expression Profiling Interactive Analysis (GEPIA) (http://gepia.cancer-pku.cn/) databases. A GSE21034 dataset with SPOCK1 expression data between tumor and normal tissues was downloaded from the Gene Expression Omnibus (GEO) database (https://www.ncbi.nlm.nih.gov/geo/). The GSE35988 dataset representing SPOCK1 expression between castration-sensitive prostate cancer (CSPC) and CRPC tissues was also retrieved from the GEO database. The most typical GO terms of the SPOCK1 gene were acquired from the ICGC Data Portal (https://dcc.icgc.org/).

2.4. Patients and clinical data

A total of 34 patients with PCa who underwent radical resection of the tumors in Shanghai Tongji Hospital of Tongji University were recruited between 2012 and 2020. Patients were selected according to the following criteria: 1) confirmation of pathological diagnosis, 2) absence of postoperative adjuvant anti-cancer therapy, and 3) reviewing TNM classification, Gleason scores, and prostate-specific antigen (PSA) levels. The clinical data of each patient were acquired from the admission records. The Medical Ethics Committee of Shanghai Tongji Hospital of Tongji University approved the study. All the study participants gave written informed consent to publish clinical details and images.

2.5. RNA isolation and reverse transcription-quantitative PCR (RT-qPCR)

The total RNA was extracted using Trizol (Sigma-Aldrich, St. Louis, MO, USA). It was reverse transcribed to cDNA with a

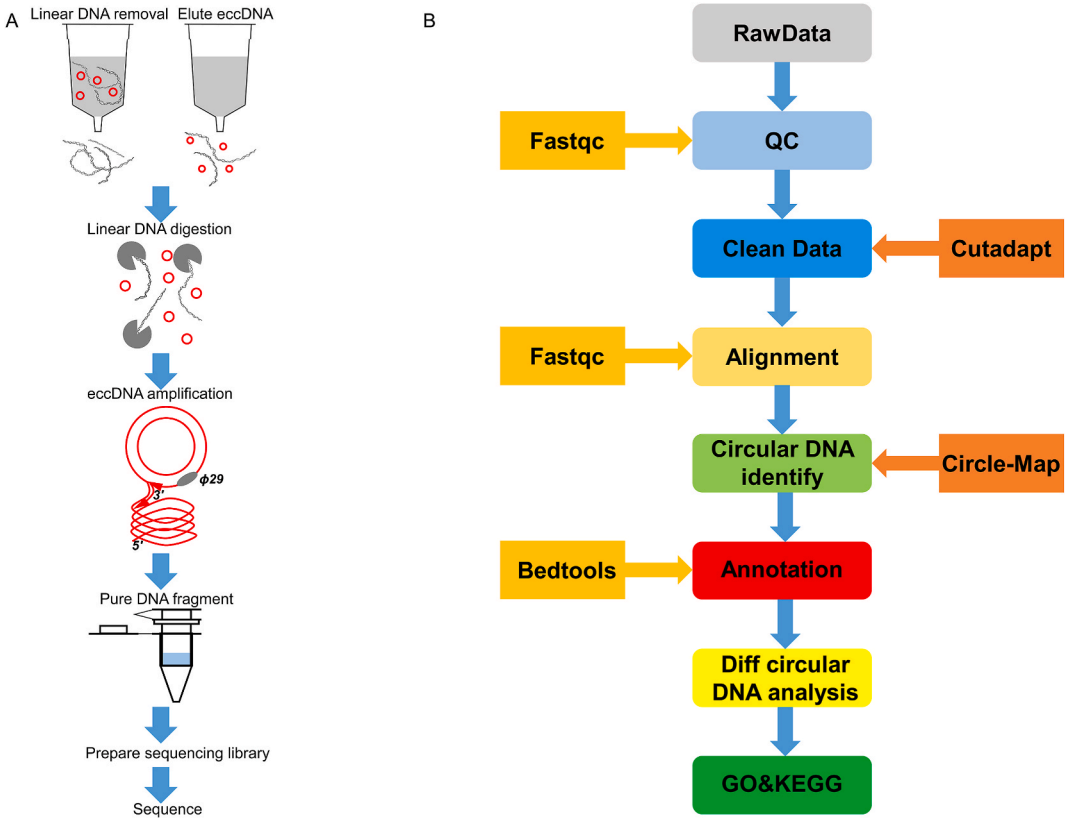

Fig. 1. Overview of Circle-seq technology and data analysis process.
(A) The Flow diagram of eccDNA purification, enrichment, and detection steps for the Circle-seq.
(B) The Flow diagram of the process of data analysis.

PrimeScript RT Reagent Kit (Takara Bio Inc., Otsu, Japan), and the cDNA was subjected to qPCR. The levels of the glyceraldehyde-3-phosphate dehydrogenase (*GAPDH*) gene served as the endogenous control, and the relative expression of the target genes was assessed using the $2^{-\Delta\Delta Ct}$ method. The qPCR primer sequences were as follows: SPOCK1: sense, 5′-CAACTGCTTGTTCCCAGAGG-3′, antisense, 5′-GCCAATGACTTCCCTATCCA-3′; E-cadherin: sense, 5′-AATCCAAAGCCTCAGGTCATAAACA-3′, antisense, 5′-TTGGGTCGTTGTACTGAATGGTC-3′; Vimentin: sense, 5′-GTTTCCCCTAAACCGCTAGG -3′, antisense, 5′-AGCGAGAGTGGCAGAGGA-3′; N-cadherin: sense, 5′-TGGATGGGCTGCCTCCAGGTGAC-3′, antisense, 5′-ACCAGCCCACCCCTCGAGCCC-3′; GAPDH: sense, 5′-GCCATCACGCCACAGTTTC-3′, antisense, 5′-ATGTCGAAGCCCCATAGTGAA-3′.

2.6. Immunohistochemistry (IHC)

The tumor tissue microarray was done according to the above description. The anti-SPOCK1 antibody (Proteintech Group, Inc., 28203-1-AP; 1:400 dilution) was used for the IHC staining. The staining intensity of the specimen was evaluated by the pathologists blinded to the clinicopathological data and the clinical results of patients. The tissue microarray was dewaxed in xylene solution, rehydrated with gradient ethanol concentrations, and subjected to antigen repair and blocking of the inactivated endogenous peroxidase. Subsequently, the anti-SPOCK1 antibody (1:400 dilution) was added, and the microarray was incubated at 4 °C overnight. The microarray was incubated for 45 min with a secondary antibody. The SPOCK1 staining intensity was scored on a 1 to 3 scale: 1, low; 2, median; and 3, high.

2.7. Statistical analysis

Statistical analysis was performed with GraphPad Prism 8.0. All values are presented as means ± standard deviation (SD). Student's *t*-test was used to determine statistical differences between two groups. And $P < 0.05$ was considered statistically significant (*: $P < 0.05$, **: $P < 0.01$, ***: $P < 0.001$; NS: no significance).

3. Results

3.1. Detection and analysis of eccDNA across various PCa tissues and cell types

The eccDNA data from 5 prostate cell lines (i.e., normal prostate RWPE-1, C4-2, 22RV1, C4-2R, and LNCaP cells), prostate tumor tissues, and normal prostate tissues was obtained with Circle-seq. The eccDNA purification, enrichment, and detection steps for the sequencing and process of data analysis were depicted in Fig. 1 (see also Materials and methods), and the eccDNA length distribution derived from the 4 PCa cell lines is shown in Fig. 2A–D. The Circle-seq results revealed that the locations of the peaks for eccDNA length varied across cell types. For instance, while the C4-2 and 22RV1 eccDNAs exhibited the highest peak at approximately 350-bp position, the C4-2R and LNCaP eccDNAs showed the highest peaks at approximately 150-bp position. Genomic distribution analysis showed that eccDNA was derived from all 23 pairs of chromosomes (Fig. 2E–H), and the frequency of eccDNA per Mb per chromosome varied substantially. In each cell line, the highest frequency was on chromosome 19, and among the sex chromosomes, the Y chromosome frequency was higher than that of the X chromosome in all cases. The exact distribution of eccDNA locations on individual chromosomes is illustrated in the eccDNA karyoplots (Fig. 2I and J), suggesting that the eccDNA quantity distributed on the sex chromosomes is relatively small across the chromosomes. The differential analysis of eccDNA formation among the PCa cell lines identified 6005 differentially expressed eccDNAs between C4-2R and C4-2 cell samples (Fig. 2K and L). In addition, compared with the Enz-sensitive cell C4-2 line, 3222 significantly differential eccDNAs were recognized in the Enz-resistant C4-2R line, with 1714 upregulated and 1508 downregulated eccDNAs (Fig. 2K and Supplementary Material 1-3). Similarly, a total of 14,728 differentially expressed eccDNAs were found between LNCaP and 22RV1 cell lines. Finally, a total of 10,112 significantly differential eccDNAs were detected between Enz-resistant C4-2R and Enz-sensitive LNCaP cell lines, with 7837 upregulated and 2275 downregulated eccDNAs (Fig. 2L). In addition, the coverage statistics were conducted on corresponding genomic elements of eccDNAs (Fig. 2M), uncovering that the eccDNA molecules of the 4 PCa cells were most enriched in gene2kbD and gene2kbU, with relatively low distributions in CpG islands. These results indicate that eccDNA generation in PCa cells is not entirely random but shows a preference for specific locations.

3.2. The GO and KEGG pathway enrichment analysis of differential eccDNA-related genes between Enz-sensitive and Enz-resistant PCa cells

Gene ontology (GO) is a public electronic tool for hierarchically classifying gene functions of gene sets using GO enrichment analysis. The Kyoto Encyclopedia of Genes and Genomes (KEGG) enrichment analysis identifies the pathways to which the genes belong and recognizes the genes that may interact to uncover the molecular mechanisms behind the phenomenon. The GO analysis demonstrated that the downregulated eccDNA-related genes in the "C4-2R vs. C4-2" dataset were involved in all 3 GO terms: biological process, cellular process, and molecular function. The most enriched functions were synapse organization, modulation of chemical synaptic transmission, and regulation of trans-synaptic signaling (Fig. 3A). Likewise, the downregulated eccDNA-related genes in the "22RV1 vs. LNCaP" dataset (Fig. 3C) were associated with similar functions. The most enriched functions of upregulated eccDNA-related genes in the "C4-2R vs. C4-2" dataset were regulation of cell morphogenesis and axonogenesis (Fig. 3B), and these were also the top functions of upregulated eccDNA-related genes in the "22RV1 vs. LNCaP" dataset (Fig. 3D). A subsequent KEGG pathway analysis uncovered the top enriched pathways for the eccDNA in the 2 datasets mentioned above. Interestingly, focal adhesion,

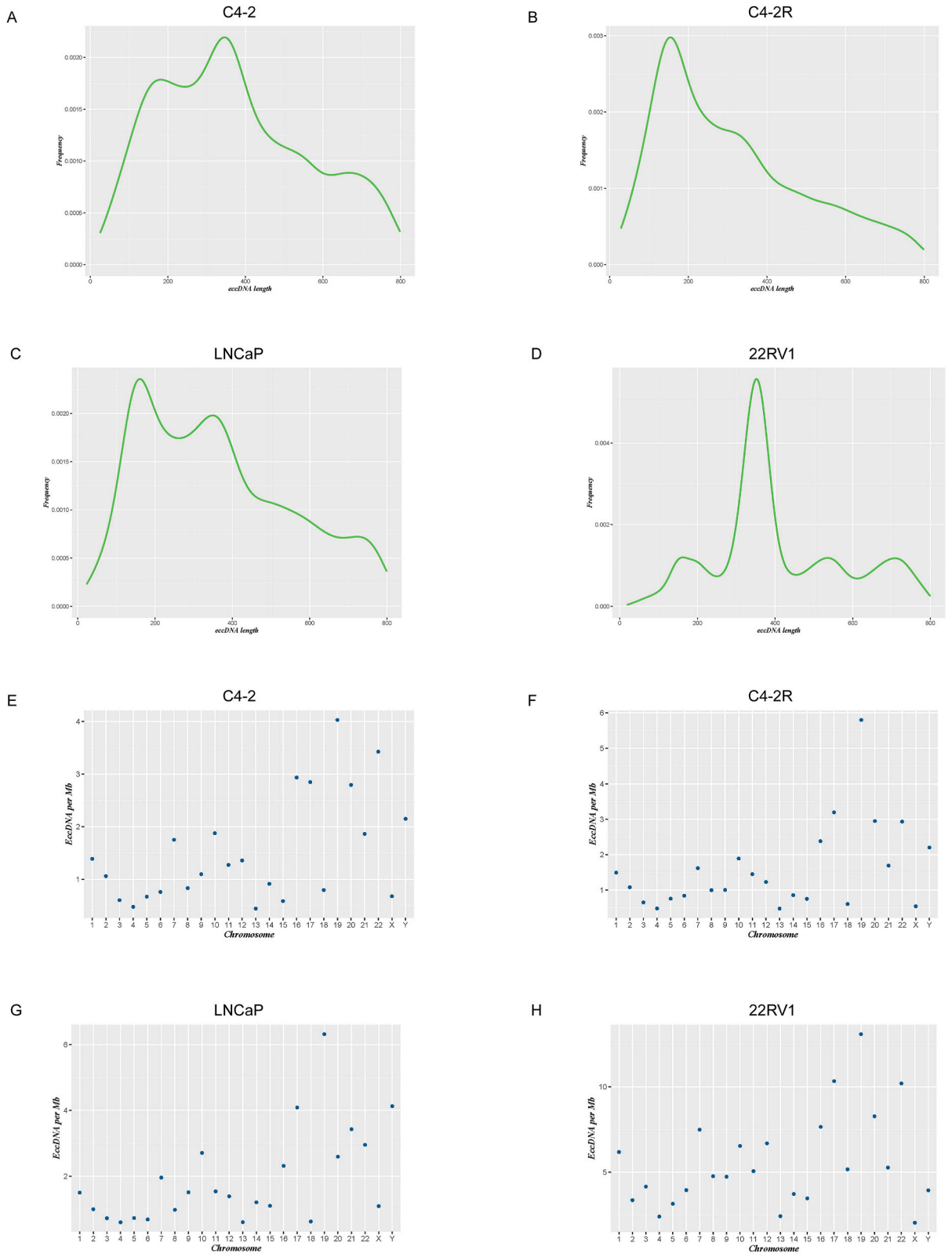

Fig. 2. General overview of sequencing results for four types of prostate cancer cells.
(A)-(D) The length distribution of eccDNA derived from the four types of cell lines.
(E)-(H) The eccDNAs production densities derived from all 23 pairs of chromosomes.

(I)-(J) The eccDNA karyoplots of the four types of cell lines.
(K) The differential analysis of eccDNA formation between C4-2R and C4-2 cells.
(L) The differential analysis of eccDNA formation between 22RV1 and LNCaP cells.
(M) The coverage statistics on corresponding genomic elements of eccDNAs among the PCa cells.

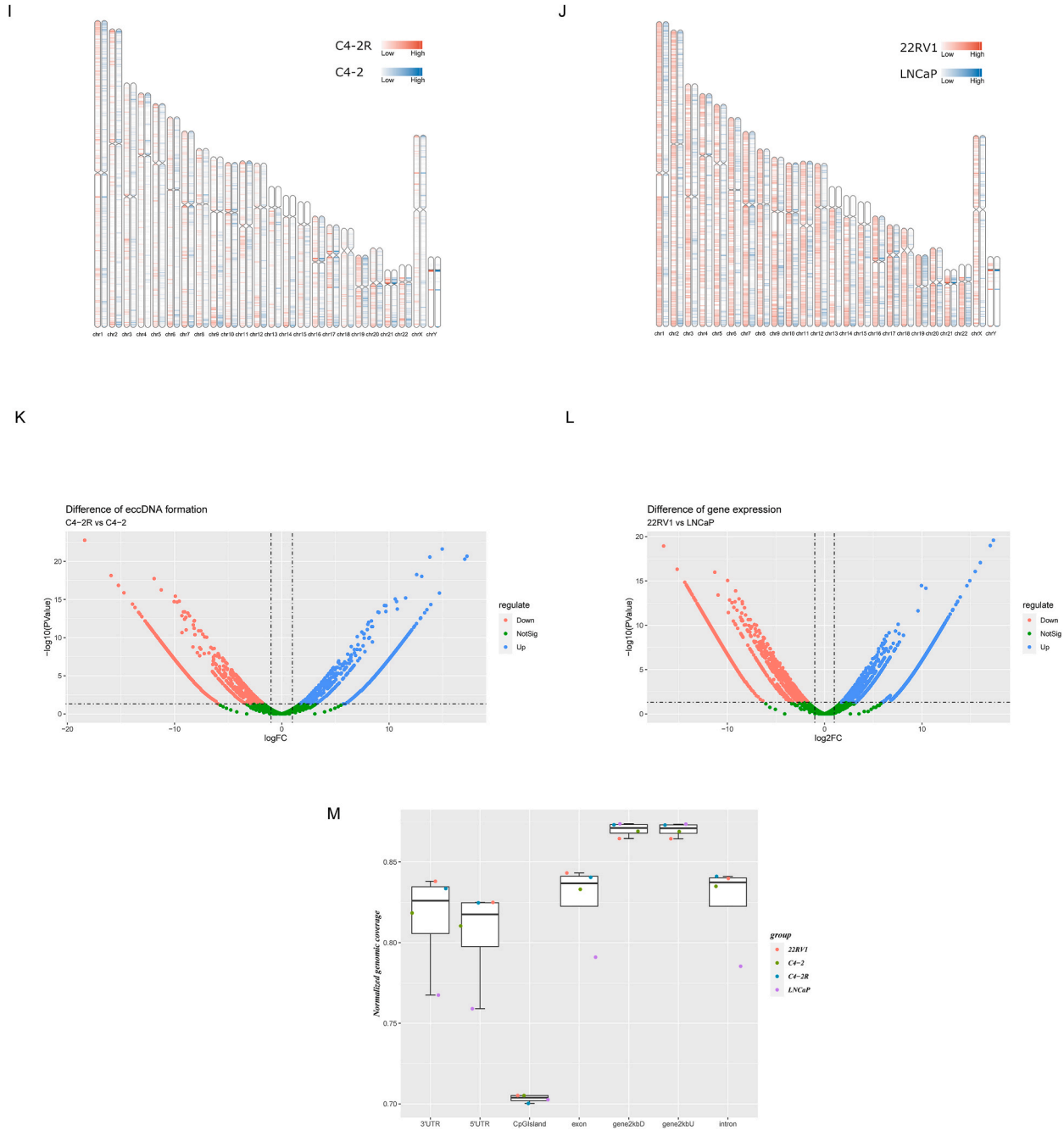

Fig. 2. (*continued*).

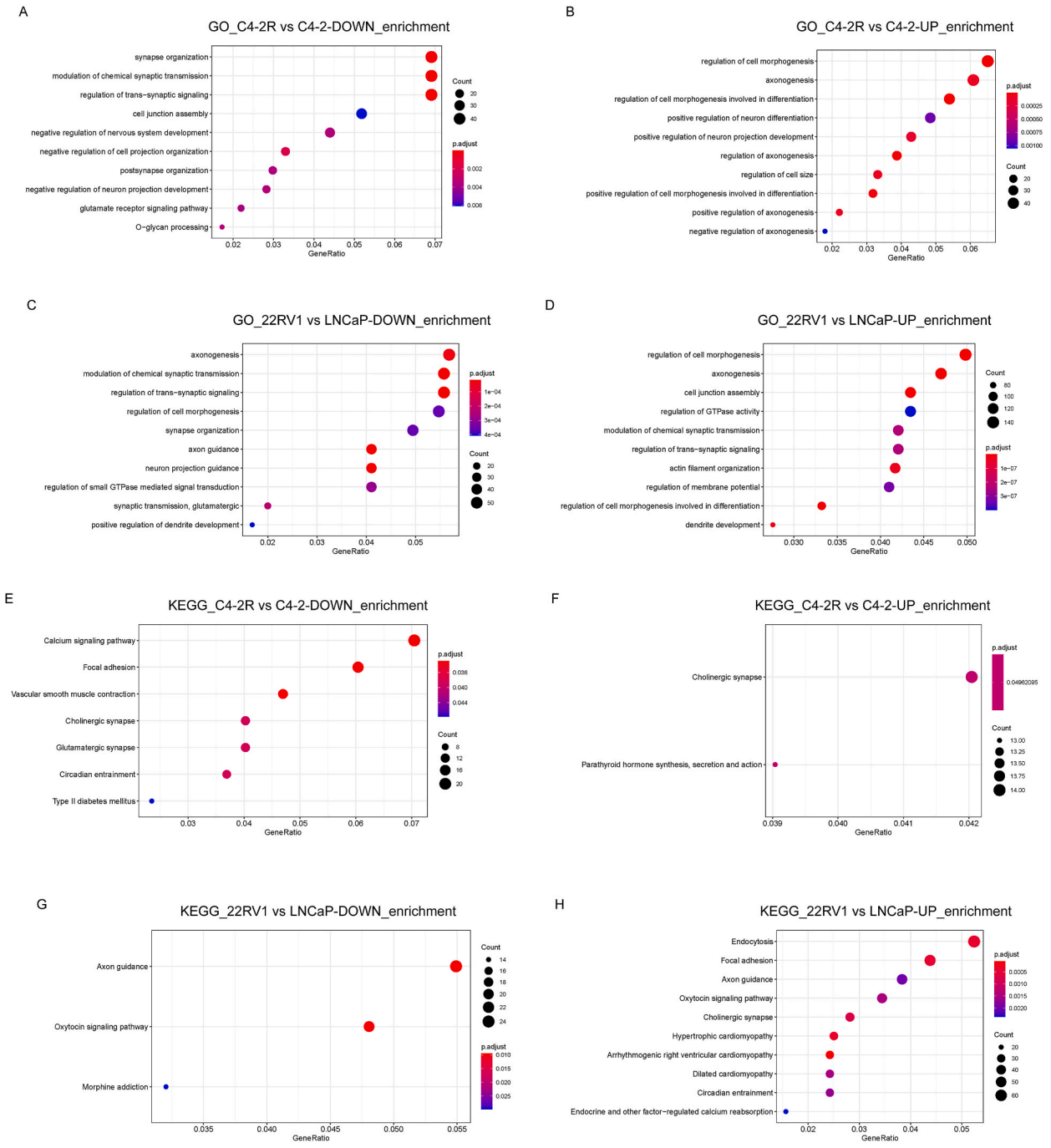

Fig. 3. The GO and KEGG pathway enrichment analysis of differential eccDNA-related genes between Enz-sensitive and Enz-resistant PCa cells.
(A)-(B) The top enriched downregulated (A) and upregulated (B) eccDNA-related genes GO terms in the "C4-2R vs. C4-2" dataset.
(C)-(D) The top enriched downregulated (C) and upregulated (D) eccDNA-related genes GO terms in the "22RV1 vs. LNCaP" dataset.
(E)-(F) The top enriched pathways of downregulated (E) and upregulated (F) eccDNA-related genes in the "C4-2R vs. C4-2" dataset in the KEGG pathway analysis.
(G)-(H) The top enriched pathways of downregulated and upregulated eccDNA-related genes in the "22RV1 vs. LNCaP" dataset in the KEGG pathway analysis.

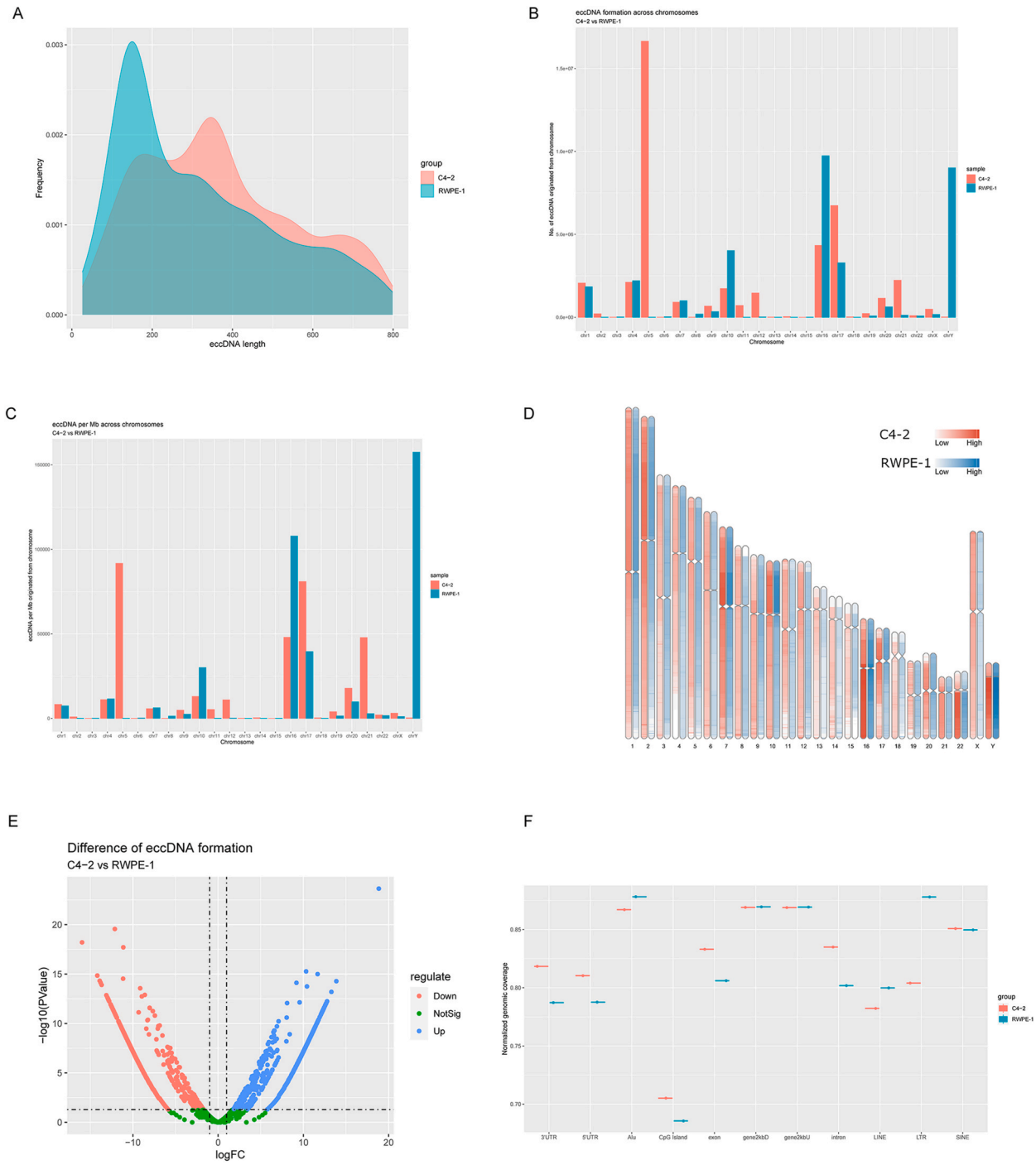

Fig. 4. Identification of differentially expressed eccDNAs and enrichment analysis of eccDNA-related genes between C4-2 and RWPE-1 cells.
(A) The length distribution of eccDNA derived from C4-2 and RWPE-1 cells.
(B) The total number of eccDNAs originated from each chromosome.
(C) The number of eccDNAs per Mb originated from each chromosome.
(D) The schematic of the eccDNAs distribution density on the chromosomes of C4-2 and RWPE-1 cells.
(E) The differential analysis of eccDNA formation between C4-2 and RWPE-1 cells.
(F) The coverage statistics of corresponding genomic elements of eccDNAs between C4-2 and RWPE-1 cells.
(G)-(H) The top enriched downregulated (G) and upregulated (H) eccDNA-related genes GO terms in the "C4-2 vs. RWPE-1" dataset.
(I)-(J) The top enriched pathways of downregulated (I) and upregulated (J) eccDNA-related genes in the "C4-2 vs. RWPE-1" dataset in the KEGG pathway analysis.

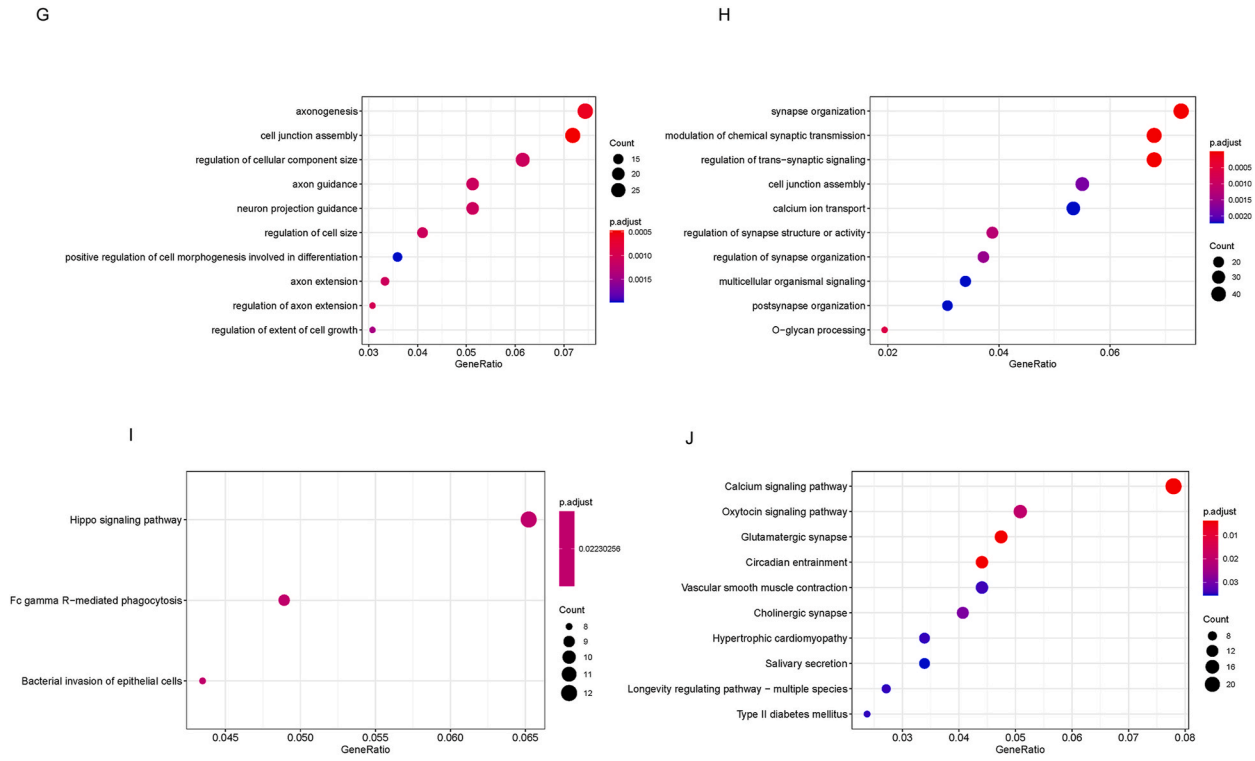

Fig. 4. (*continued*).

cholinergic synapse, axon guidance, and oxytocin signaling pathways were shared between upregulated and downregulated eccDNA-related gene datasets (Fig. 3E–H).

3.3. Identification of differentially expressed eccDNAs and enrichment analysis of eccDNA-related genes between Enz-sensitive and normal prostate cells

The length distribution of eccDNA derived from the Enz-sensitive C4-2 and prostate hyperplasia RWPE-1 cells is shown in Fig. 4A. Similar to C4-2R and LNCaP cells, the peak lengths in RWPE-1 cells were also distributed close to the 200-bp location, clearly distinguishable from C4-2 cells. In addition, the total number of eccDNAs and the number of eccDNAs per Mb originated from each chromosome (Fig. 4B and C). Furthermore, eccDNAs in C4-2 cells were most commonly formed from chromosome 5 and were more than 3 times more abundant than the number of eccDNAs produced by other chromosomes (the second most common origin was chromosome 17). By contrast, eccDNAs in RWPE-1 cells most frequently originated from chromosome 16 and also from the Y chromosome, more abundant than on the other chromosomes (Fig. 4B). Similarly, eccDNAs per Mb in C4-2 cells most commonly originated from chromosomes 5 and 17. Conversely, this distribution was not observed in RWPE-1 cells, where eccDNAs per Mb again formed from the Y chromosome, followed by chromosome 16, a clear distinction from the results of the total number distribution (Fig. 4C). A more intuitive schematic of the eccDNA distribution density on the chromosomes of the 2 cells are illustrated in Fig. 4D. Additionally, the highest density of eccDNA distribution in RWPE-1 cells was on chromosome 16 and the Y chromosome. The differential analysis uncovered 3307 differentially expressed eccDNAs between C4-2 and RWPE-1 cell samples, revealing 2452 significantly differential eccDNAs in C4-2 cells versus RWPE-1 cells, of which 1514 were upregulated eccDNAs and 938 were downregulated (Fig. 4E and Supplementary Material 4-6).

Subsequently, the coverage statistics were conducted on corresponding genomic elements of eccDNAs (Fig. 4F) to assess whether eccDNA origin is arbitrary. The eccDNA molecules in all the RWPE-1 cells were most enriched in Alu elements and long terminal repeat (LTR) sequences, with relatively lowest distributions in CpG islands, strikingly different from the eccDNA distribution positions in C4-2 cells. Again, these data imply that eccDNA generation in the cells is not entirely random but prefers specific positions on chromosomal DNA. The GO analysis showed that the most significant functions of downregulated eccDNA-related genes in the “C4-2 vs. RWPE-1” dataset were associated with axonogenesis, cell junction assembly, and regulation of cellular component size (Fig. 4G). Likewise, the most represented functions of upregulated eccDNA-related genes in the “C4-2 vs. RWPE-1” dataset were related to synapse organization, modulation of chemical synaptic transmission, and trans-synaptic signaling (Fig. 4H). Furthermore, the KEGG pathway analysis showed that the most enriched pathways of downregulated and upregulated eccDNA-related genes in the “C4-2 vs RWPE-1” dataset were the Hippo and calcium signaling pathways (Fig. 4I and J). Therefore, the above results overlap with or are partially similar to those associated with the “C4-2R vs. C4-2” dataset (Fig. 3).

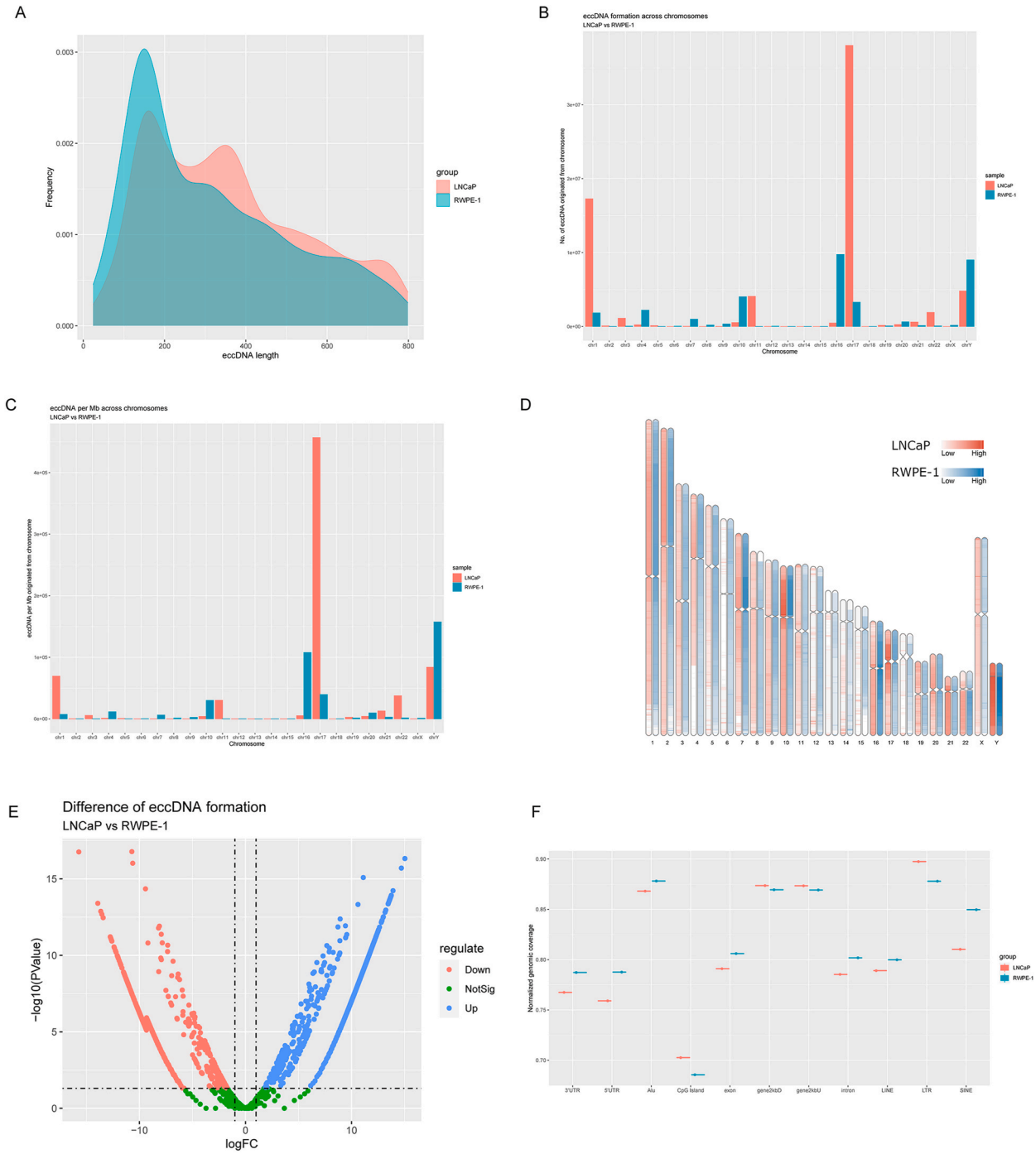

Fig. 5. Identification of differentially expressed eccDNAs and enrichment analysis of eccDNA-related genes between LNCaP and RWPE-1 cells.
(G) The length distribution of eccDNA derived from LNCaP and RWPE-1 cells.
(H) The total number of eccDNAs originated from each chromosome.
(I) The number of eccDNAs per Mb originated from each chromosome.
(J) The schematic of the eccDNAs distribution density on the chromosomes of LNCaP and RWPE-1 cells.
(K) The differential analysis of eccDNA formation between LNCaP and RWPE-1 cells.
(L) The coverage statistics of corresponding genomic elements of eccDNAs between LNCaP and RWPE-1 cells.
(G)-(H) The top enriched downregulated (G) and upregulated (H) eccDNA-related genes GO terms in the "LNCaP vs. RWPE-1" dataset.
(I)-(J) The top enriched pathways of downregulated (I) and upregulated (J) eccDNA-related genes in the "LNCaP vs. RWPE-1" dataset in the KEGG pathway analysis.

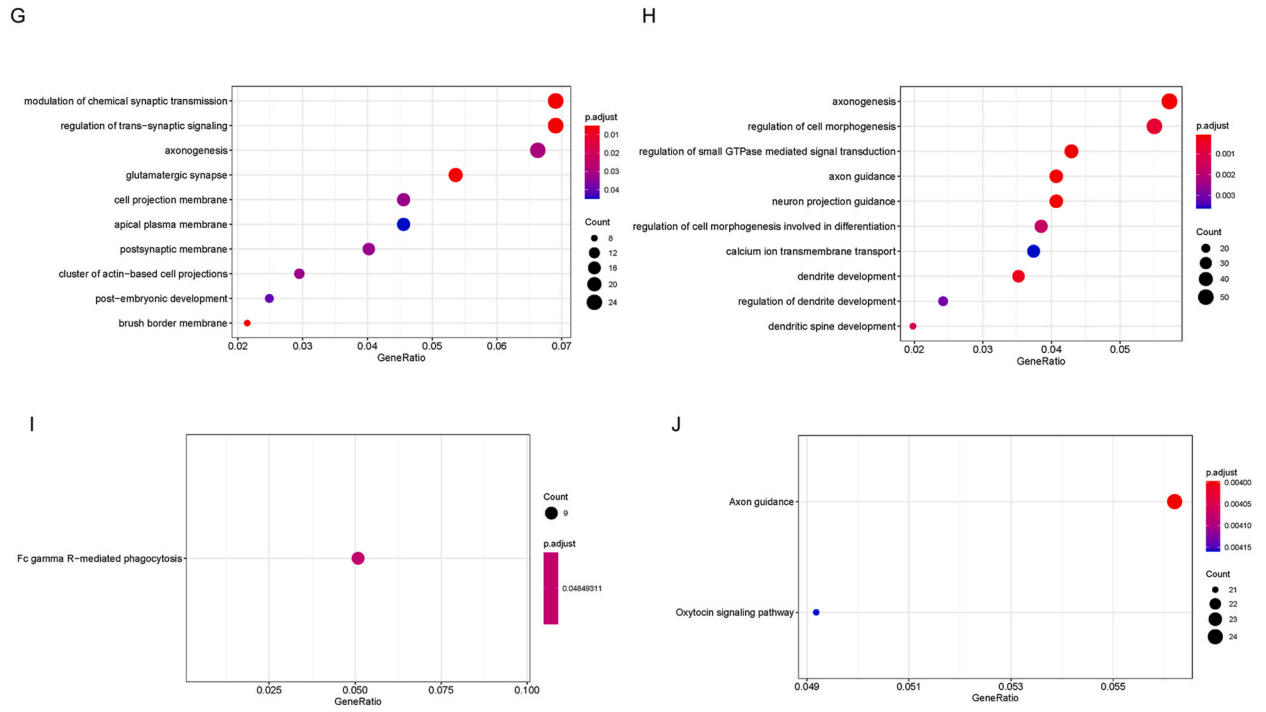

Fig. 5. (*continued*).

The comparison of the sequencing data of prostate hyperplasia RWPE-1, LNCaP, and castration-sensitive PCA cells is given in Fig. 5, and the length distribution of eccDNA derived from LNCaP and RWPE-1 cells is shown in Fig. 5A. In LNCaP cells, 2 peaks of closer proximity with the higher one located close to 200 bp were observed and were quite different from those in C4-2 cells. Moreover, peak values of the total number of eccDNAs and the number of eccDNAs per Mb originated from each chromosome in LNCaP cells (Fig. 5B and C) were significantly higher than those in the C4-2 (Fig. 4B and C). The eccDNAs in the LNCaP cells most commonly originated from chromosome 17, with a peak height 2-fold higher than that of the peak located on chromosome 5 in C4-2 cells and more than 3-fold higher than that of the peak situated on chromosome 16 in RWPE-1 cells (Fig. 5B). The eccDNAs per Mb in LNCaP cells also most commonly originated from chromosome 17, with a peak height 4 times higher than that of the peak located on chromosome 5 in C4-2 cells and more than 3 times higher than that of the peak located on the Y chromosome in RWPE-1 cells (Fig. 5C). A more intuitive schematic of the eccDNA distribution density on the chromosomes of the 2 cells is visualized in Fig. 5D. The differential eccDNA analysis disclosed 3054 significantly different eccDNAs between LNCaP and RWPE-1 cells, with 2139 upregulated and 915 downregulated eccDNAs (Fig. 5E). The eccDNA molecules of the LNCaP cells were most enriched in LTR sequences, with relatively lowest distributions in the CpG islands, somewhat different from the eccDNA distribution position noted in C4-2 cells (Fig. 5F). The GO analysis showed that the most significant functions of downregulated eccDNA-related genes in the "LNCaP vs. RWPE-1" dataset were modulation of chemical synaptic transmission and regulation of trans-synaptic signaling (Fig. 5G). Similarly, the most frequent functions of upregulated eccDNA-related genes in the "LNCaP vs. RWPE-1" dataset were axonogenesis and morphogenesis (Fig. 5H). Hence, these findings showed a slight similarity to the data captured by Circle-seq in the "C4-2R vs. C4-2" dataset (Fig. 3). Finally, the KEGG pathway analysis revealed that the most enriched pathways of downregulated and upregulated eccDNA-related genes in the "LNCaP vs. RWPE-1" dataset were Fc gamma R-mediated phagocytosis and axon guidance (Fig. 5I and J).

3.4. Identification of differentially expressed eccDNAs and enrichment analysis of eccDNA-related genes between prostate tumor and normal prostate tissues

In addition to profiling prostate cells with Circle-seq, prostate tissue specimens were sequenced to clarify the eccDNA distribution in vivo. Samples A, B, and C were prostate tumor tissue specimens (Treatment group), while samples C, D, and E were normal prostate tissue specimens (Control group). The length distribution of eccDNA derived from PCa and normal prostate tissues is shown in Fig. 6A and Supplementary Figs. 1A–F. Surprisingly, the trend of eccDNA length distribution in PCa tissues was remarkably consistent with that in normal prostate tissues, with a peak at about 150 bp. The number of eccDNAs per Mb originated from each chromosome (Fig. 6B and Supplementary Figs. 2A–E), and the density distribution of eccDNAs formed in each specimen did not show a clear pattern of bias. The peaks in the eccDNA distribution in several tumor tissues appeared at chromosomes 7, 8, or 20 (Fig. 6B and Supplementary Figs. 2A–B), whereas the peaks in several normal prostate tissues appeared at chromosomes 3, 12, or 20 (Supplementary Figs. 2C–F). A more intuitive schematic of the eccDNA distribution density on the chromosomes of the 2 groups is presented in Fig. 6C. The left side of

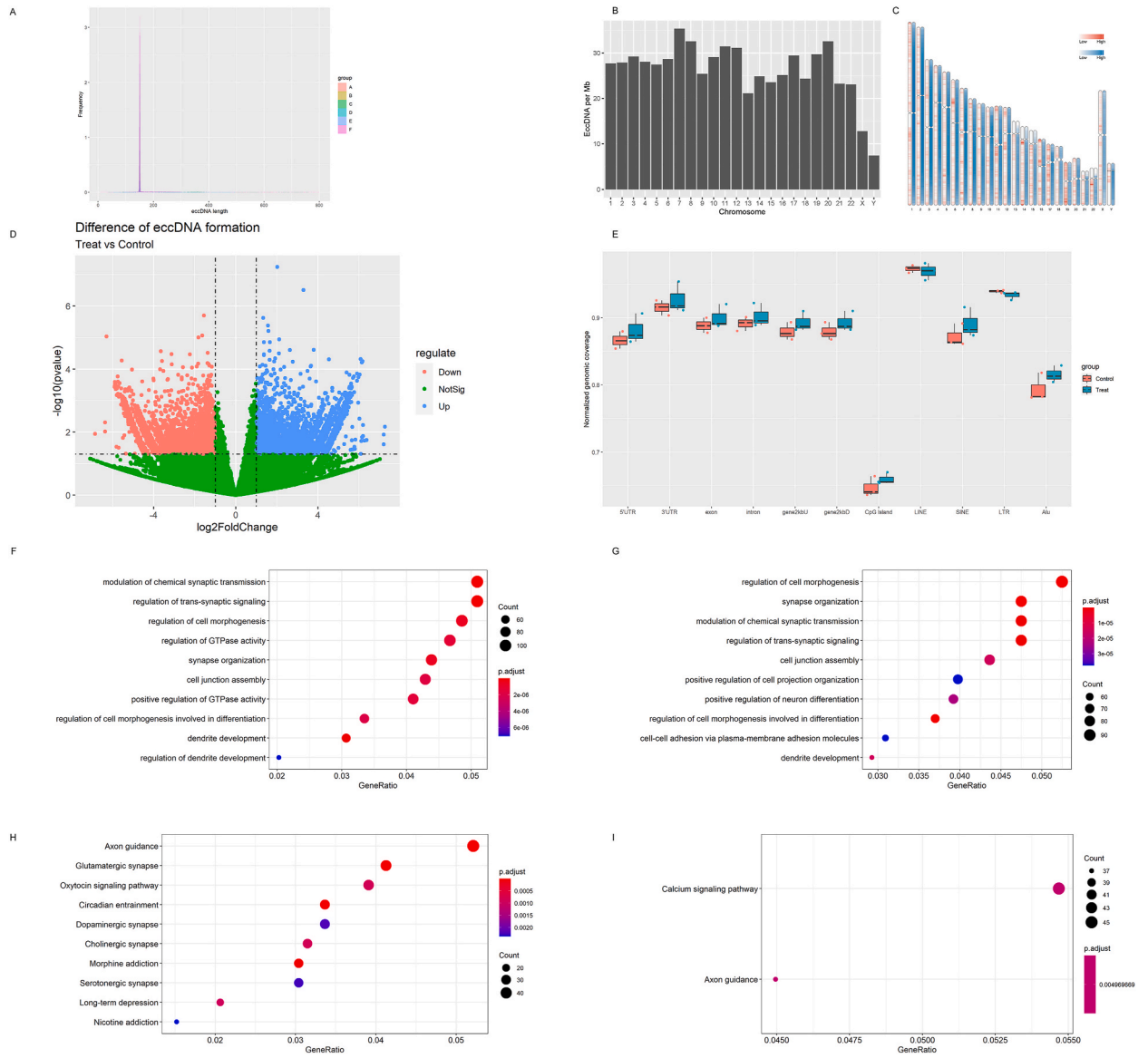

Fig. 6. Identification of differentially expressed eccDNAs and enrichment analysis of eccDNA-related genes between prostate tumor and normal prostate tissues.
(A) The length distribution of eccDNA derived from PCa and normal prostate tissues.
(B) The number of eccDNAs per Mb originated from each chromosome in Samples A.
(C) The schematic of the eccDNA distribution density on the chromosomes between Treatment and Control group.
(D) The differential analysis of eccDNA formation between Treatment and Control group.
(E) The coverage statistics of corresponding genomic elements of eccDNAs between Treatment and Control group.
(F)-(G) The top enriched downregulated (F) and upregulated (G) eccDNA-related genes GO terms in the "Treat vs. Control" dataset.
(H)-(I) The top enriched pathways of downregulated (H) and upregulated (I) eccDNA-related genes in the "Treat vs. Control" dataset in the KEGG pathway analysis.

each set of chromosomes showed the gene density and the right side showed the density of individual intervals on the chromosomes forming eccDNAs in 500-kb units. A total of 12,111 significantly different eccDNAs were detected in the Treatment group compared with the Control group, with 5645 upregulated and 6466 downregulated eccDNAs (Fig. 6D and Supplementary Material 7-9). The results of eccDNA genomic coverage analysis in PCa and normal tissues showed high similarity, uncovering the highest enrichment in both groups was in long interspersed nuclear elements (LINEs) and the lowest in CpG islands (Fig. 6E). The GO analysis revealed that the most significant functions of downregulated eccDNA-related genes in the "Treat vs. Control" dataset were modulation of chemical synaptic transmission and regulation of trans-synaptic signaling (Fig. 6F). Likewise, the most frequent function of upregulated eccDNA-related genes in the "Treat vs. Control" dataset was regulation of cell morphogenesis (Fig. 6G). Finally, the KEGG pathway

analysis showed that the most significant pathways of downregulated and upregulated eccDNA-related genes in the "Treat vs. Control" dataset were axon guidance and calcium signaling pathways (Fig. 6H and I).

3.5. Identification of eccDNA-related target genes with the highest correlation with PCa development and Enz-resistance

We performed a few analyses on several Circle-seq datasets to explore the role of upregulated eccDNA in PCa and the relevant target genes. We overlapped the upregulated parts of 3 datasets: "C4-2 vs. RWPE-1," "LNCaP vs. RWPE-1," and "Treat vs. Control" (Fig. 7A), to identify the eccDNA-related target genes with the highest correlation with PCa development in vitro and in vivo. The results uncovered 6 overlapping eccDNA-related genes: leucine rich repeat containing G protein-coupled receptor 6 (LGR6), protein kinase cAMP-dependent type I regulatory subunit beta (PRKAR1B), calneuron 1 (CALN1), EF-hand calcium binding domain 6 (EFCAB6), PTPRN2, and SPOCK1 (Table 1). Next, we retrieved their differential expression between PCa and normal tissues from TCGA database to verify that the TCGA expression of these genes matches that of our Circle-seq data. The results showed that only SPOCK1 and PTPRN2 genes were significantly upregulated in the PCa group compared with the control group, while the rest were relatively downregulated or insignificantly affected (Fig. 7B–G).

Therefore, given the inconsistency in the sequencing results, we downloaded the relevant expression data from the GEPIA platform to validate SPOCK1 and PTPRN2 expression in PCa. For both genes, the transcript density and degree of expression reflected significant differences between PCa and normal tissues, with SPOCK1 expression in PCa the highest among all tumors (Fig. 7H–K).

Next, we overlapped the "C4-2 vs. RWPE-1," "C4-2R vs. C4-2," and "Treat vs. Control" datasets to highlight the eccDNA-related target genes upregulated in PCa and normal groups and Enz-resistant and Enz-sensitive groups (Fig. 8A). We discovered 5 genes meeting this requirement: zinc finger protein 423 (ZNF423); microtubule associated monooxygenase, calponin and LIM domain containing 3 (MICAL3); CUGBP Elav-like family member 4 (CELF4); hook microtubule tethering protein 2 (HOOK2); and SPOCK1 (Table 2). Comparing their expression with that in TCGA database showed that only SPOCK1 and HOOK2 were significantly upregulated in the PCa versus the control group (Figs. 7E and 8B–E). However, the data from the GEPIA platform demonstrated that the transcript density and degree of expression of the HOOK2 gene did not show significant differences in PCa and normal tissues (Fig. 8F and G), suggesting inconsistencies in HOOK2 expression between the 2 data sources. In conclusion, because SPOCK1 is the only consistent gene appearing after 2 overlap analyses (Fig. 8H), it is likely an eccDNA-associated target gene crucial for PCa development and drug resistance. The eccDNAs associated with SPOCK1 in each of the datasets from the sequencing results were shown in Table 3.

3.6. Extrachromosomal circular DNA-associated SPOCK1 contributes to PCa occurrence and drug resistance

The SPOCK1 gene is a typical oncogene, and its protein is an ECM proteoglycan that affects tumor progression by regulating ECM remodeling. It promotes drug resistance, proliferation, and metastasis in various tumors. By analyzing the ICGC Data Portal, we discovered that the most significant GO terms of SPOCK1 involved calcium ion binding, postsynaptic density, cell adhesion, and regulation of cell growth. Concomitantly, these terms strongly agreed with the highly enriched GO terms in our Circle-seq results. Next, we explored the GEO database to determine the role of SPOCK1 in prostate carcinogenesis and drug resistance. The PCa-related GSE21034 dataset was downloaded from the GEO database to assess SPOCK1 differential expression between normal and tumor tissues, and the GSE35988 dataset was retrieved for the same analysis between CSPC and CRPC tissues. The SPOCK1 expression levels were significantly higher in the tumor group than in the normal group ($P = 0.001$), implying SPOCK1 is a central gene in CRPC development (Fig. 9A). Similarly, its expression was substantially enhanced in the CRPC group compared with the CSPC group (Fig. 9B), confirming SPOCK1 expression between the datasets.

Subsequently, we performed IHC staining to detect the expression of the SPOCK1 protein in PCa tissues and validate its expression in PCa. We assigned SPOCK1-stained tissue specimens into 4 groups based on the staining intensity from weak to strong: Negative (Normal), Score = 1 (Low), Score = 2 (Median), and Score = 3 (High) (Fig. 9C). The scoring revealed that a positive SPOCK1 signal positively correlated with PSA levels ($P = 0.0326$) (Fig. 9D), tumor stages ($P = 0.0325$) (Fig. 9E), and Gleason scores ($P = 0.0076$) (Fig. 9F) but had no significant correlation with metastasis ($P = 0.5798$) (Fig. 9G). These data suggest that the SPOCK1 protein plays a vital role in PCa progression.

We also conducted Western blotting to verify SPOCK1 protein expression in 5 prostate cell lines: prostatic hyperplasia RWPE-1, Enz-sensitive PCa (C4-2 and LNCaP), and Enz-resistant PCa (C4-2R and 22RV1) cells. The blots showed that SPOCK1 expression in C4-2 cells was significantly higher than in RWPE-1 cells. Its expression was also notably higher in C4-2R cells than in C4-2 cells (Fig. 9H) (Supplementary Material 10). Likewise, SPOCK1 expression in LNCaP cells was significantly higher than that in RWPE-1 cells, and it was markedly higher in 22RV1 cells than in LNCaP cells (Fig. 9I) (Supplementary Material 10). Quantifying SPOCK1 expression with RT-qPCR showed that the SPOCK1 protein expression in these cell lines matched that of the SPOCK1 mRNA (Fig. 9J and K), confirming the Western blotting data.

In summary, the results revealed that SPOCK1 was highly expressed in PCa and promoted Enz resistance process.

3.7. SPOCK1 promotes PCa development and Enz-resistance through EMT mechanism

Evidence suggests that SPOCK1 promotes EMT, enhancing drug resistance, proliferation, and metastasis in many cancers. Since EMT is a fundamental process during tumorigenesis and progression, we sought to determine the SPOCK1 effects on EMT in prostate hyperplasia RWPE-1 and PCa cells. We quantified the levels of 3 EMT marker mRNA (i.e., N-cadherin, E-cadherin, and Vimentin) in the 2 cell lines with Western blot and qPCR. A large number of studies had demonstrated that lack of E-cadherin expression and increased

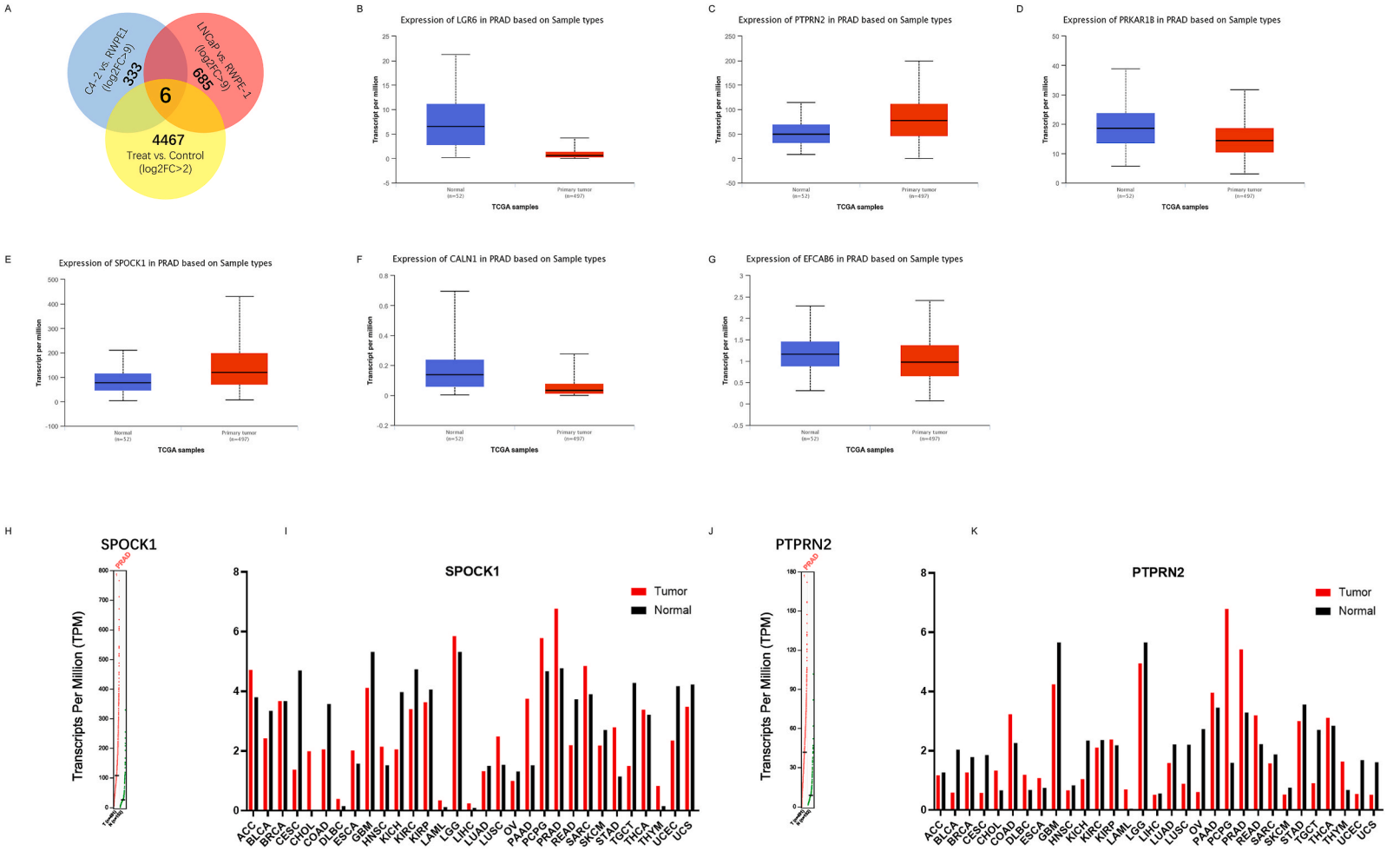

Fig. 7. Identification of eccDNA-related target genes with the highest correlation with PCa development.
(A) There were 6 repeating eccDNA-related target genes in the overlapping of 3 datasets ("C4-2 vs. RWPE-1," "LNCaP vs. RWPE-1," and "Treat vs. Control").
(B)-(G) The differential expression of LGR6 (B), PTPRN2 (C), PRKAR1B (D), SPOCK1 (E), CALN1 (F) and EFCAB6 (G) between PCa and normal tissues from TCGA database.
(H) The transcript density of SPOCK1 between PCa and normal tissues from GEPIA.
(I) The degree of expression reflected significant differences of SPOCK1 between PCa and normal tissues from GEPIA.
(J) The transcript density of PTPRN2 between PCa and normal tissues from GEPIA.
(K) The degree of expression reflected significant differences of PTPRN2 between PCa and normal tissues from GEPIA.

Table 1
The 6 repeating eccDNA-related target genes and their corresponding eccDNA in the overlapping of the datasets "C4-2 vs. RWPE-1," "LNCaP vs. RWPE-1," and "Treatment vs. Control".

	C4-2 vs. RWPE-1	LNCaP vs. RWPE-1	Treat vs. Control
LGR6	eccDNA_242	eccDNA_270	eccDNA_26922
PTPRN2	eccDNA_2894	eccDNA_3428	eccDNA_358238
PRKAR1B	eccDNA_2723	eccDNA_3172	eccDNA_335176
SPOCK1	eccDNA_2556	eccDNA_2965	eccDNA_302693
CALN1	eccDNA_2794	eccDNA_3267	eccDNA_345545
EFCAB6	eccDNA_2207	eccDNA_2549	eccDNA_227364

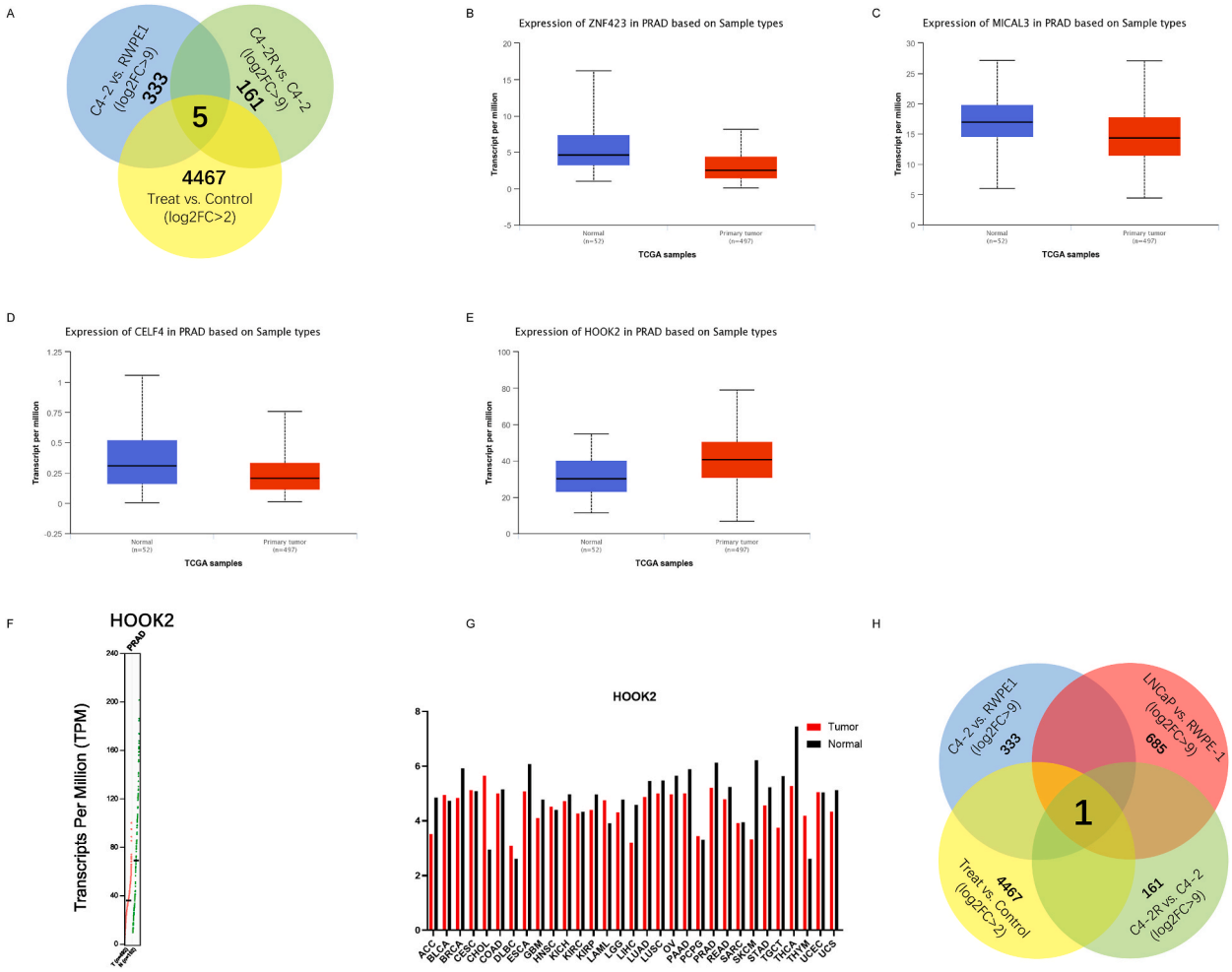

Fig. 8. Identification of eccDNA-related target genes with the highest correlation with Enz-resistance.
(A) There were 5 repeating eccDNA-related target genes in the overlapping of 3 datasets ("C4-2 vs. RWPE-1," "C4-2R vs. C4-2" and "Treat vs. Control").
(B)-(E) The differential expression of ZNF423 (B), MICAL3 (C), CELF4 (D) and HOOK2 (E) between PCa and normal tissues from TCGA database.
(F) The transcript density of HOOK2 between PCa and normal tissues from GEPIA.
(G) The degree of expression reflected significant differences of HOOK2 between PCa and normal tissues from GEPIA.
(H) SPOCK1 was the only one repeating eccDNA-related target gene in the overlapping of 4 datasets ("C4-2 vs. RWPE-1," "C4-2R vs. C4-2", "LNCaP vs. RWPE-1", and "Treat vs. Control").

expression of N-cadherin and Vimentin were hallmarks of epithelial-mesenchymal transition (EMT) and were associated with an increased risk of cancer development and progression [21–23]. We found that the protein expression of N-cadherin and Vimentin increased sequentially in RWPE-1 cells, Enz-sensitive, and Enz-resistant PCA cells, while that of E-cadherin decreased sequentially in these cells (Fig. 10A and B) (Supplementary Material 11). Similar results could be seen in mRNA expression (Fig. 10C–H). Next, we

Table 2
The 5 repeating eccDNA-related target genes and their corresponding eccDNA in the overlapping of the datasets "C4-2 vs. RWPE-1," "C4-2R vs. C4-2," and "Treatment vs. Control".

	C4-2 vs. RWPE-1	C4-2R vs. C4-2	Treat vs. Control
SPOCK1	eccDNA_2556	eccDNA_13160	eccDNA_302693
MICAL3	eccDNA_2133	eccDNA_10830	eccDNA_223605
CELF4	eccDNA_1450	eccDNA_7638	eccDNA_160175
HOOK2	eccDNA_1553	eccDNA_8211	eccDNA_167585
ZNF423	eccDNA_1116	eccDNA_6116	eccDNA_138088

Table 3
The eccDNAs associated with SPOCK1 in each of the datasets from Circle-seq results.

	Chr	Location		Length	Dataset
		Start	End		
eccDNA_2556	chr5	137211642	137212155	513	C4-2 vs. RWPE-1
eccDNA_2965	chr5	137581089	137581586	497	LNCaP vs. RWPE-1
eccDNA_302693	chr5	137230101	137230251	150	Treat vs. Control
eccDNA_13160	chr5	137518567	137524102	5535	C4-2R vs. C4-2
eccDNA_13158	chr5	137134851	137135411	560	LNCaP vs. 22RV1

performed IHC staining to verify the expression of the 3 EMT markers in the normal and PCa tissues. Indeed, N-cadherin and Vimentin expression in PCa tissues was higher than in normal ones, while that of E-cadherin was lower (Fig. 10I–K). In addition, we investigated whether changes in SPOCK1 expression affect the expression of the 3 EMT markers to clarify the relationship between the effects of SPOCK1 on PCa and EMT mechanisms. To this end, we examined the protein expression in C4-2 cells under SPOCK1 overexpression, discovering that SPOCK1 represses E-cadherin but induces Vimentin and N-cadherin expression in Enz-sensitive PCa cells (Fig. 10L) (Supplementary Material 12).

In conclusion, these findings show that the positive SPOCK1-mediated regulation of prostate carcinogenesis and progression is closely related to the EMT mechanism.

4. Discussion

Extrachromosomal circular DNA (eccDNA) is a type of circular DNA originating from chromosomes but is likely independent of them. Because of its structural properties, it has potential extensive applications as a new biomarker for cancer prevention and treatment [24–26]. Although eccDNA has been reported in multiple cancers, such as leukemia [27], gastric [28], ovarian cancer [29], oropharyngeal [30], breast cancer [31,32], and colorectal cancers [33], few studies are known on prostate cancer. In this study, we used Circle-seq and studied the distribution pattern and level of eccDNA expression across various PCa cell lines and tissues. We confirmed that eccDNA is a common mutational element in PCa and identified an eccDNA-related target gene SPOCK1. We found that SPOCK1 was highly expressed in PCa cancer tissues and cells and exists as eccDNA in PCa, promoting its development and drug resistance through the EMT mechanism.

We identified SPOCK1 as a target gene owing to the Circle-seq method, which obtains a comprehensive picture of the overall landscape of eccDNA sizes and content in cell populations. We sequenced 5 groups of samples: 4 groups of cell samples and 1 group of clinical tissue samples. The main objective of the sequencing was to disclose eccDNA and its associated target genes that differed most markedly between normal and PCa cells and tissues, as well as between castration-sensitive and castration-resistant PCa cells. We also used the sequencing to explore more detailed information, such as the length distribution of eccDNAs in each group of samples, the frequency distribution of eccDNAs in each chromosome, the number of differentially expressed eccDNAs in each group and the corresponding degree of differentiation, the distribution of eccDNAs in each genome element, and the GO and KEGG pathways highly enriched by differentially expressed eccDNAs in each group.

We discovered that the length of most eccDNAs in normal prostate RWPE-1 cells was shorter than that in PCa cells and that the height of their frequency peaks was about 200 bp smaller than that of eccDNAs in PCa cells. In addition, we observed that the number of eccDNAs from each chromosome between normal and PCa cells differed considerably. The eccDNAs in RWPE-1 cells originated most frequently from chromosomes 16 and Y, while those in PCa cells were formed from chromosomes 5 and 17. In addition, no significant biased difference was found in the coverage statistics of eccDNA across genomic elements in normal and tumor cells. However, PCa cells tended to have more eccDNAs with upregulated genes than downregulated compared with normal prostate cells. The length distributions, the number from each chromosome, and the coverage statistics across genomic elements of eccDNAs in various PCa cells showed no significant differences. We also found no significant differences in the length of eccDNA, its frequency on each chromosome, or its distribution on genomic elements between PCa and normal tissues. By employing GO and KEGG analyses, we uncovered the functions and pathways highly enriched in up- and downregulated differentially expressed eccDNA-associated genes between tumor and normal tissues: synapse organization, modulation of chemical synaptic transmission, regulation of trans-synaptic signaling, axon guidance, and calcium signaling pathway.

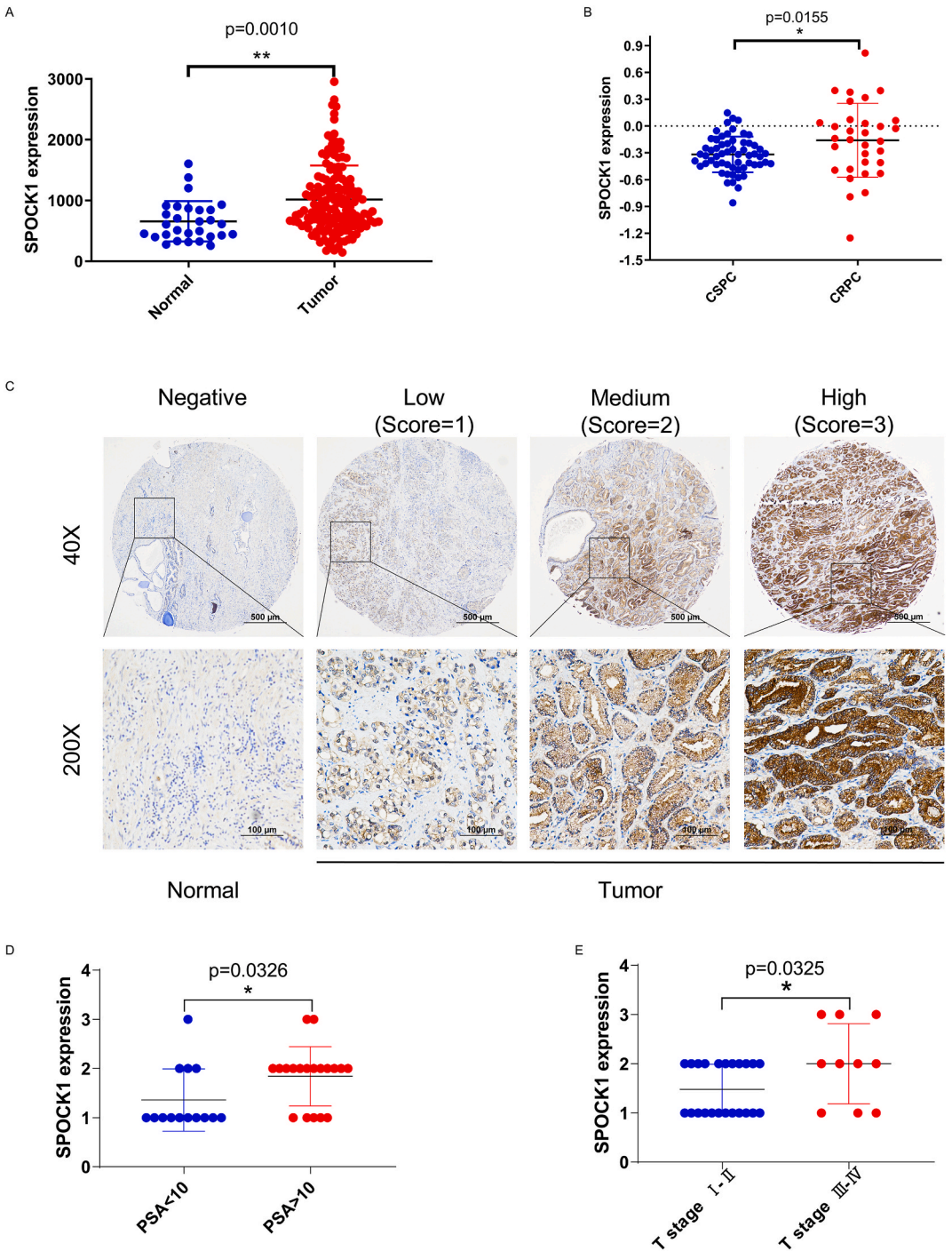

Fig. 9. eccDNA-associated SPOCK1 contributes to PCa occurrence and drug resistance.
(A) The differential analysis of SPOCK1 gene expression levels between PCa and normal tissues from dataset GSE21034.
(B) The differential analysis of SPOCK1 gene expression levels between CSPC and CRPC tissues from dataset GSE35988.
(C) Representative SPOCK1 staining divided into Negative and Score 1–3 based on staining intensity from weak to strong in PCa tissues.
(D)-(G) The correlation of SPOCK1 expression level with PSA (D), T stages (E), Gleason scores (F) and metastasis (G).
(H) SPOCK1 protein expression in C4-2 cells was significantly higher than in RWPE-1 cells. Its expression was also notably higher in C4-2R cells than in C4-2 cells.
(I) SPOCK1 protein expression in LNCaP cells was significantly higher than that in RWPE-1 cells. Its expression was also notably higher in 22RV1 cells than in LNCaP cells.
(J) SPOCK1 mRNA expression in C4-2 cells was significantly higher than in RWPE-1 cells. Its expression was also notably higher in C4-2R cells than

in C4-2 cells.
(K) SPOCK1 mRNA expression in LNCaP cells was significantly higher than that in RWPE-1 cells. Its expression was also notably higher in 22RV1 cells than in LNCaP cells.

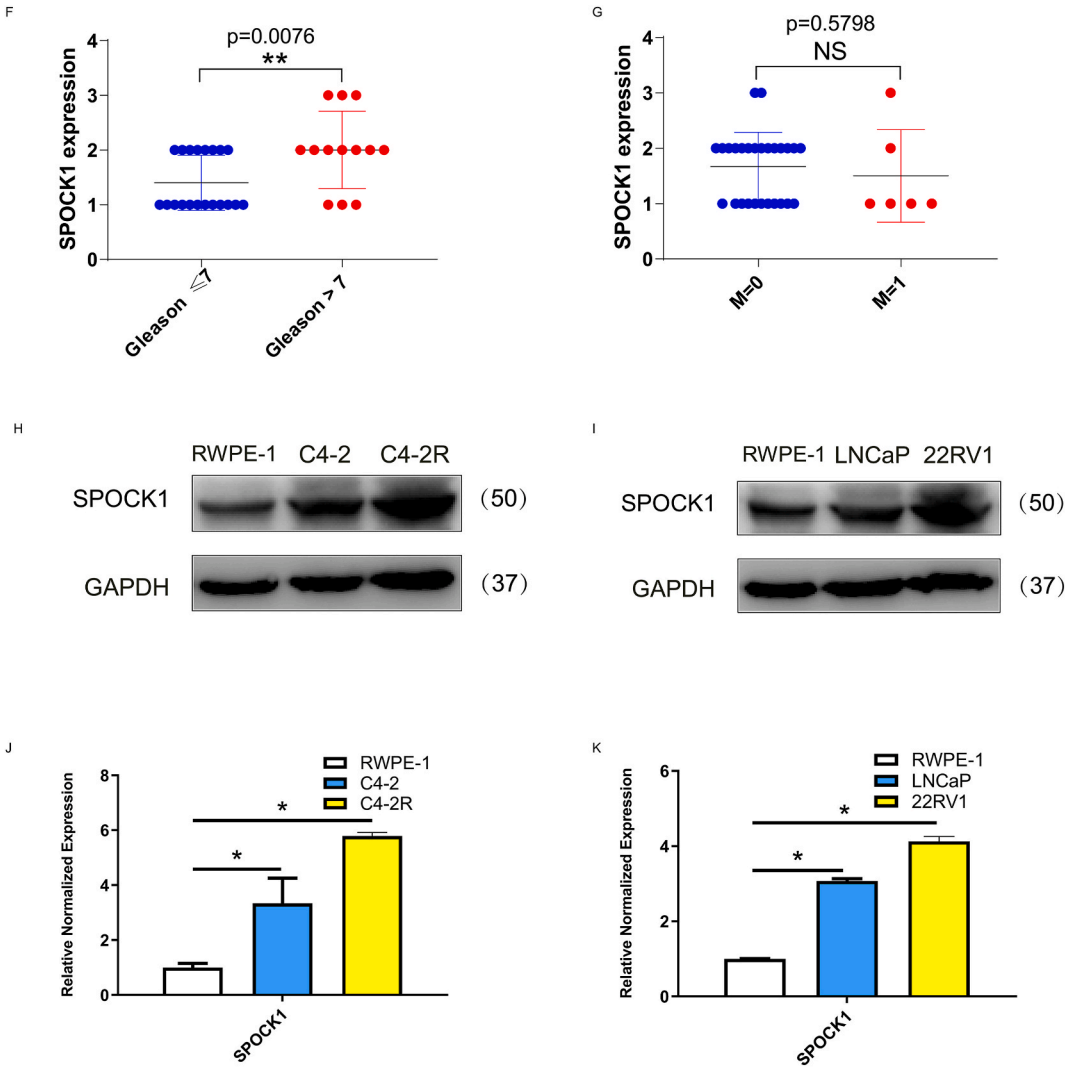

Fig. 9. (*continued*).

Ultimately, by overlapping the sequencing datasets and combing them with bioinformatics analysis, we discovered that the SPOCK1 gene is the most significant and consistent differentially expressed eccDNA-associated target gene between PCa and healthy tissues. Moreover, our bioinformatics analysis showed that the GO and KEGG-enriched genes and pathways related to SPOCK1 in publicly available databases agreed with those in our Circle-seq results.

SPOCK1 was reportedly associated with the proliferation and drug resistance of tumor cells [34]. In addition, SPOCK1, which related to EMT mechanism, could serve as a potential prognostic and therapeutic biomarker for a variety kinds of cancers [35,36]. Epithelial-mesenchymal transition (EMT) was known as the process of the transdifferentiation of epithelial cells into motile mesenchymal cells [37]. EMT has been shown to promote tumorigenesis by enhancing proliferation, invasion and resistance to apoptosis. In addition, EMT-derived tumor cells acquired stem cell properties and exhibited significant therapeutic resistance [38]. Given these features, the biological processes of EMT had been widely recognized as key hallmarks of carcinogenesis and drug resistance, and targeting the EMT pathway constitutes a cancer therapeutic strategy with great potential [39,40]. There had been many reports confirming that EMT played important roles in the progression of various cancers, such as colorectal cancer, breast cancer and lung cancer [41,42].

Our series of experimental analyses on tissues and cells confirmed significant differences in the protein and mRNA expression of SPOCK1 between prostate normal and tumor cells. Importantly, these differences were also apparent between Enz-sensitive and Enz-resistant tumor cells. Therefore, these in vitro findings validate the sequencing results to some extent. Finally, we verified that SPOCK1

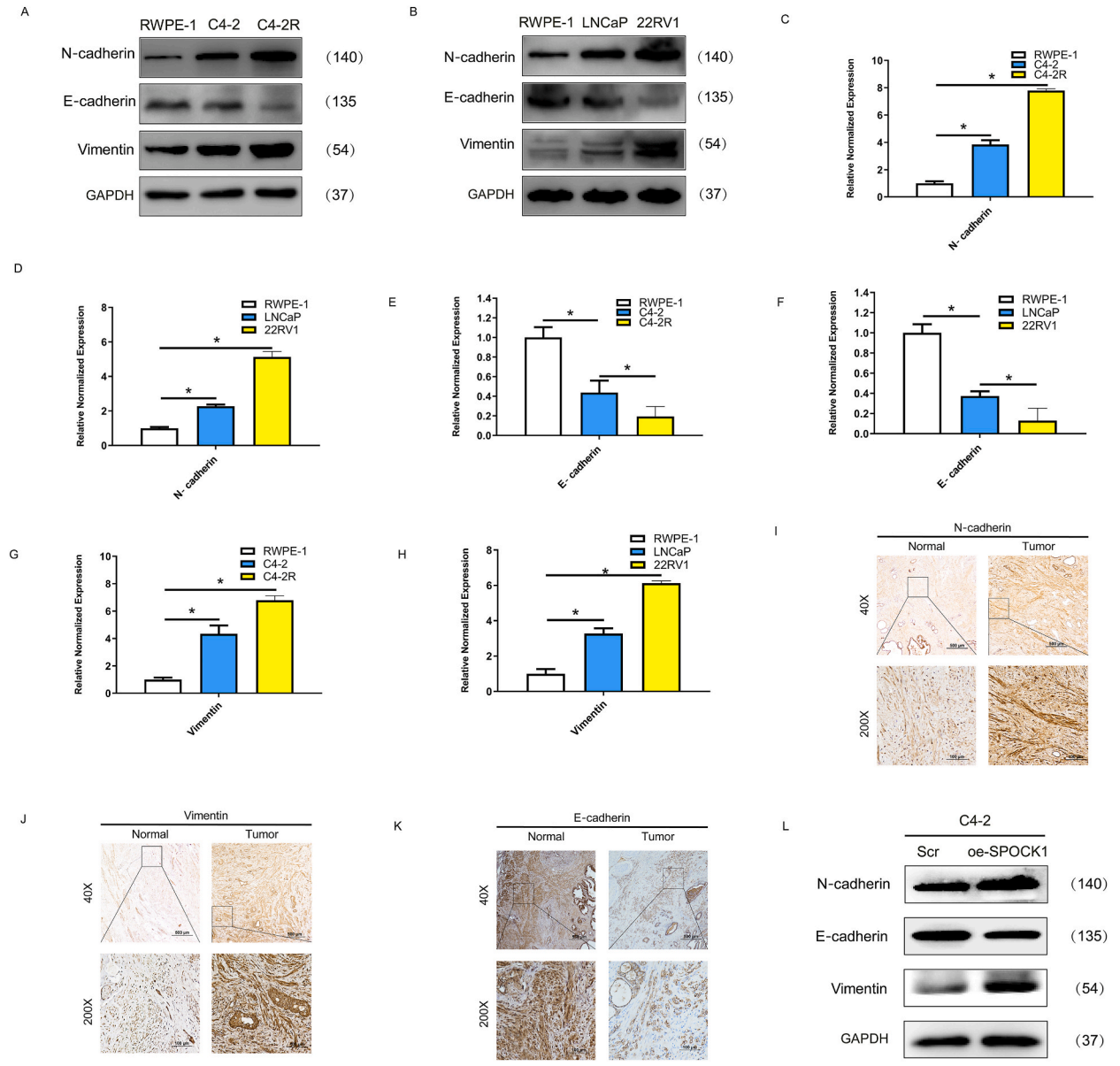

Fig. 10. SPOCK1 promotes PCa development and Enz-resistance through EMT mechanism.
(A) The protein expression of N-cadherin and Vimentin increased sequentially in RWPE-1, C4-2, and C4-2R, while E-cadherin decreased sequentially.
(B) The protein expression of N-cadherin and Vimentin increased sequentially in RWPE-1, LNCaP, and 22RV1, while E-cadherin decreased sequentially.
(C)-(H) The mRNA expression of N-cadherin(C) and Vimentin(G) increased sequentially in RWPE-1, C4-2, and C4-2R, while E-cadherin(E) decreased sequentially. Meanwhile, mRNA expression of N-cadherin(D) and Vimentin(H) increased sequentially in RWPE-1, LNCaP, and 22RV1, while E-cadherin(F) decreased sequentially.
(I)-(K) N-cadherin (I) and Vimentin (J) expression in PCa tissues was higher than in normal ones, while that of E-cadherin (K) was lower.
(L) N-cadherin and Vimentin protein expression in C4-2 increased obviously after overexpressing SPOCK1, while E-cadherin decreased.

action affecting PCa development and drug resistance was positively correlated to the EMT mechanism.

In conclusion, SPOCK1 is an eccDNA in prostate cancer and promotes PCa development and Enz resistance through the EMT mechanism. Our results suggest that upregulated genes in the form of eccDNA are oncogenes in PCa and play a pivotal role in carcinogenesis. They also indicate that identifying highly expressed genes in the form of eccDNA and their mechanisms of action may provide new strategies for treating this disease.

Although our study offers valuable novel insights into human eccDNA, it has certain drawbacks. For instance, the way eccDNA

regulates the SPOCK1 target gene and the specific linkage site is not experimentally verified. Therefore, we plan to address these unresolved questions in our subsequent studies and further understanding of this gene as a potential treatment target in PCa.

Ethics statement

The Ethics Committee of Tongji Hospital affiliated to Tongji University examined and approved the studies relating to human participants. The ethical approval referenced number was SBKT-2024-106.

Funding

This study was supported by the National Natural Science Foundation of China (Grant No. 81672526, 81802560), Natural Science Foundation of Shanghai Municipal Science and Technology Committee (No. 22ZR1456-800) and Key disciplines of Tongji Hospital. None of these study sponsors had any role in the study design, collection, analysis, and interpretation of data.

Data availability statement

The authors confirmed that the data supporting the findings of this study were available within the article and its supplementary materials. The Circle-Seq data associated with this study would be deposited into a publicly available repository when accepted.

CRediT authorship contribution statement

Yicong Yao: Writing – original draft, Visualization, Validation, Software, Methodology, Investigation, Formal analysis. **Qinghua Wang:** Visualization, Formal analysis, Data curation. **Wei Jiang:** Validation, Supervision, Data curation. **Haopeng Li:** Investigation. **Xilei Li:** Investigation. **Tong Zi:** Investigation. **Xin Qin:** Investigation. **Yan Zhao:** Investigation. **Denglong Wu:** Writing – review & editing, Supervision, Conceptualization. **Gang Wu:** Writing – review & editing, Resources, Project administration, Methodology, Funding acquisition, Conceptualization.

Declaration of competing interest

The authors announced that the study was carried out without any commercial or financial relationships that could be interpreted as a potential conflict of interest.

Appendix A. Supplementary data

Supplementary data to this article can be found online at https://doi.org/10.1016/j.heliyon.2024.e37075.

References

[1] G. Zhang, Z. Zhang, Y. Pei, et al., Biological and clinical significance of radiomics features obtained from magnetic resonance imaging preceding pre-carbon ion radiotherapy in prostate cancer based on radiometabolomics, Front. Endocrinol. 14 (2023) 1272806.
[2] R.L. Siegel, K.D. Miller, A. Jemal, Cancer statistics, 2018, CA A Cancer J. Clin. 68 (1) (2018).
[3] M.C.S. Wong, W.B. Goggins, H.H.X. Wang, et al., Global incidence and mortality for prostate cancer: analysis of temporal patterns and trends in 36 countries, Eur. Urol. 70 (5) (2016) 862–874.
[4] L. Bennett, P.K. Jaiswal, R.V. Harkless, et al., Glucocorticoid receptor (GR) activation is associated with increased cAMP/PKA signaling in castrate-resistant prostate cancer, Mol. Cancer Therapeut. 23 (4) (2024) 552–563.
[5] S. Li, Y. Kang, Y. Zeng, Targeting tumor and bone microenvironment: novel therapeutic opportunities for castration-resistant prostate cancer patients with bone metastasis, Biochim. Biophys. Acta Rev. Canc (2023) 189033.
[6] X. Ling, Y. Han, J. Meng, et al., Small extrachromosomal circular DNA (eccDNA): major functions in evolution and cancer, Mol. Cancer 20 (1) (2021) 113.
[7] S. Ren, D. Wu, X. Shen, et al., Deciphering the role of extrachromosomal circular DNA in adipose stem cells from old and young donors, Stem Cell Res. Ther. 14 (1) (2023) 341.
[8] J. Ye, P. Huang, K. Ma, et al., Genome-wide extrachromosomal circular DNA profiling of paired hepatocellular carcinoma and adjacent liver tissues, Cancers 15 (22) (2023).
[9] W. Lv, X. Pan, P. Han, et al., Circle-Seq reveals genomic and disease-specific hallmarks in urinary cell-free extrachromosomal circular DNAs, Clin. Transl. Med. 12 (4) (2022) e817.
[10] Y. Yang, Y. Yang, H. Huang, et al., PLCG2 can exist in eccDNA and contribute to the metastasis of non-small cell lung cancer by regulating mitochondrial respiration, Cell Death Dis. 14 (4) (2023) 257.
[11] H.D. Mller, Circle-Seq: Isolation and sequencing of chromosome-derived circular DNA elements in cells, Methods Mol. Biol. 2119 (2020) 165–181.
[12] S.Q. Tsai, N.T. Nguyen, J. Malagon-Lopez, et al., CIRCLE-seq: a highly sensitive in vitro screen for genome-wide CRISPR-Cas9 nuclease off-targets, Nat. Methods 14 (6) (2017) 607–614.
[13] D. Gerovska, M.J. Ara Zo-Bravo, Systemic lupus erythematosus patients with DNASE1L3-Deficiency have a distinctive and specific genic circular DNA profile in plasma, Cells 12 (7) (2023).
[14] K. Wen, L. Zhang, Y. Cai, et al., Identification and characterization of extrachromosomal circular DNA in patients with high myopia and cataract, Epigenetics 18 (1) (2023) 2192324.
[15] J. Pang, X. Pan, L. Lin, et al., Characterization of plasma extrachromosomal circular DNA in gouty arthritis, Front. Genet. 13 (2022) 859513.

[16] Z. Ye, J. Chen, X. Hu, et al., SPOCK1: a multi-domain proteoglycan at the crossroads of extracellular matrix remodeling and cancer development, Am. J. Cancer Res. 10 (10) (2020) 3127–3137.
[17] F. Yu, G. Li, J. Gao, et al., SPOCK1 is upregulated in recurrent glioblastoma and contributes to metastasis and Temozolomide resistance, Cell Prolif. 49 (2) (2016) 195–206.
[18] Y.-W. Lin, Y.-C. Wen, C.-H. Hsiao, et al., Proteoglycan SPOCK1 as a poor prognostic marker promotes malignant progression of clear cell renal cell carcinoma via triggering the snail/Slug-MMP-2 Axis-mediated epithelial-to-mesenchymal transition, Cells 12 (3) (2023).
[19] X. Cui, Y. Wang, W. Lan, et al., SPOCK1 promotes metastasis in pancreatic cancer via NF-κB-dependent epithelial-mesenchymal transition by interacting with IκB-α, Cell. Oncol. 45 (1) (2022) 69–84.
[20] H.-X. Liu, Y.-Y. Cao, J.-Y. Qu, SPOCK1 promotes the proliferation and migration of colon cancer cells by regulating the NF-κB pathway and inducing EMT, Neoplasma 68 (4) (2021) 702–710.
[21] M. Li, X. Wang, X. Chen, et al., GK921, a transglutaminase inhibitor, strengthens the antitumor effect of cisplatin on pancreatic cancer cells by inhibiting epithelial-to-mesenchymal transition, Biochim. Biophys. Acta, Mol. Basis Dis. 1870 (2) (2023) 166925.
[22] P. Wang, K. Tong, Y. Li, et al., The role and mechanism of HIF-1α-mediated glypican-3 secretion in hypoxia-induced tumor progression in hepatocellular carcinoma, Cell. Signal. (2023) 111007.
[23] L. Zhu, Q. Zeng, J. Wang, et al., Cathepsin V drives lung cancer progression by shaping the immunosuppressive environment and adhesion molecules cleavage, Aging (Albany NY) 15 (2023).
[24] T. Guo, G.-Q. Chen, X.-F. Li, et al., Small extrachromosomal circular DNA harboring targeted tumor suppressor gene mutations supports intratumor heterogeneity in mouse liver cancer induced by multiplexed CRISPR/Cas9, Genome Med. 15 (1) (2023) 80.
[25] C.R. Dos Santos, L.B. Hansen, M. Rojas-Triana, et al., Variation of extrachromosomal circular DNA in cancer cell lines, Comput. Struct. Biotechnol. J. 21 (2023) 4207–4214.
[26] W. Lu, Y. Wang, T. Luo, et al., Identification and global characterization of eccDNA reveals hallmarks in iron nanoparticles-treated breast cancer cells, Genes Dis 11 (2) (2024) 532–534.
[27] T. Zeng, W. Huang, L. Cui, et al., The landscape of extrachromosomal circular DNA (eccDNA) in the normal hematopoiesis and leukemia evolution, Cell Death Dis. 8 (1) (2022) 400.
[28] X. Jiang, X. Pan, W. Li, et al., Genome-wide characterization of extrachromosomal circular DNA in gastric cancer and its potential role in carcinogenesis and cancer progression, Cell. Mol. Life Sci. 80 (7) (2023) 191.
[29] Y. Zhang, K. Dong, X. Jia, et al., A novel extrachromosomal circular DNA related genes signature for overall survival prediction in patients with ovarian cancer, BMC Med. Genom. 16 (1) (2023) 140.
[30] J. Pang, N. Nguyen, J. Luebeck, et al., Extrachromosomal DNA in HPV-mediated oropharyngeal cancer drives diverse oncogene transcription, Clin. Cancer Res. 27 (24) (2021) 6772–6786.
[31] Y. Ouyang, W. Lu, Y. Wang, et al., Integrated analysis of mRNA and extrachromosomal circular DNA profiles to identify the potential mRNA biomarkers in breast cancer, Gene 857 (2023) 147174.
[32] L. Yang, M. Wang, X.E. Hu, et al., EccDNA-oriented ITGB7 expression in breast cancer, Ann. Transl. Med. 10 (24) (2022) 1344.
[33] Y. Chen, Q. Qiu, J. She, et al., Extrachromosomal circular DNA in colorectal cancer: biogenesis, function and potential as therapeutic target, Oncogene 42 (13) (2023) 941–951.
[34] Y. Xu, P. Zhao, X. Xu, et al., T790M mutation sensitizes non-small cell lung cancer cells to radiation via suppressing SPOCK1, Biochem Biophys Rep 38 (2024) 101729.
[35] Y. Liu, T. Han, J. Wu, et al., SPOCK1, as a potential prognostic and therapeutic biomarker for lung adenocarcinoma, is associated with epithelial-mesenchymal transition and immune evasion, J. Transl. Med. 21 (1) (2023) 909.
[36] X. Li, Y. Gu, B. Hu, et al., A liquid biopsy assay for the noninvasive detection of lymph node metastases in T1 lung adenocarcinoma, Thorac Cancer 15 (16) (2024) 1312–1319.
[37] W. Jia, Z. Huang, L. Zhou, et al., Purinergic signalling in cancer therapeutic resistance: from mechanisms to targeting strategies, Drug Resist. Updates 70 (2023) 100988.
[38] S. Lamouille, J. Xu, R. Derynck, Molecular mechanisms of epithelial-mesenchymal transition, Nat. Rev. Mol. Cell Biol. 15 (3) (2014) 178–196.
[39] V. Mittal, Epithelial mesenchymal transition in tumor metastasis, Annu. Rev. Pathol. 13 (2018) 395–412.
[40] A. Dongre, R.A. Weinberg, New insights into the mechanisms of epithelial-mesenchymal transition and implications for cancer, Nat. Rev. Mol. Cell Biol. 20 (2) (2019) 69–84.
[41] N. Zhang, A.S. Ng, S. Cai, et al., Novel therapeutic strategies: targeting epithelial-mesenchymal transition in colorectal cancer, Lancet Oncol. 22 (8) (2021) e358–e368.
[42] I. Akrida, F. Mulita, K.-M. Plachouri, et al., Epithelial to mesenchymal transition (EMT) in metaplastic breast cancer and phyllodes breast tumors, Med. Oncol. 41 (1) (2023) 20.